

# **Air System Management for Fuel Cell Vehicle Applications**

By

JOSHUA MICHAEL CUNNINGHAM  
B.S. (Michigan State University) 1996

THESIS

Submitted in partial satisfaction of the requirements for the degree of

MASTER OF SCIENCE

In

Transportation Technology & Policy

in the

OFFICE OF GRADUATE STUDIES

of the

UNIVERSITY OF CALIFORNIA

DAVIS

Approved:

\_\_\_\_\_ (Chair)

\_\_\_\_\_

\_\_\_\_\_

Committee in Charge

2001

## TABLE OF CONTENTS

Abstract:.....	iv
Acknowledgments: .....	vi
Nomenclature:.....	vii
<b>Part I: Background</b> .....	<b>1</b>
1.1 Introduction: Context of the air supply in the fuel cell system .....	1
1.2 Physical system configuration .....	3
1.3 Modeling the Air Supply System Components .....	6
Compressor Relationships:.....	6
Expander Relationships:.....	7
Combined Relationships: .....	8
Fuel Cell Stack Relationships: .....	9
1.4 Mathematical modeling: A summary .....	10
Performance Maps.....	10
The Air Supply Model.....	12
The Optimization between the Air System and the Fuel Cell Stack.....	13
1.5 Technology options and applicable system configurations .....	14
Current Air Supply Developers.....	14
<b>Part II: Model Studies and Simulations</b> .....	<b>17</b>
2.1 Use of an expander (turbine) .....	17
Abstract .....	17
Conclusions .....	18
2.2 High pressure vs. low pressure system operation.....	20

Abstract .....	21
Conclusions .....	22
2.3 Corrections for ambient conditions and geometry .....	23
Abstract .....	24
Conclusion.....	27
2.4 Air system transients .....	28
<b>Part III: Closing remarks.....</b>	<b>30</b>
3.1 Conclusion.....	30
3.2 Future research .....	31
<b>Part IV: APPENDIX.....</b>	<b>32</b>
4.1 References .....	32
4.2 Full copies of referenced papers from Part II.....	35
4.2.1 Expander Implications:  EVS-17 Conference 2000 .....	35
4.2.2 High-Pressure vs. Low-Pressure:  SAE World Congress 2001 .....	56
4.2.3 Air Supply Model Characteristics:  SAE FTT Conference 1999.....	76

## Abstract:

Research and development of fuel cell systems for multiple applications has dramatically increased in the past few years. The vehicular application of the fuel cell system as the powertrain leads to a number of unique challenges, namely physical packaging within the vehicle, durability and operation under extreme environmental conditions, and demanding duty cycles that include high peak power requirements and a rapid response time.

The focus of this research is on the air management system of the fuel cell powertrain in the vehicular application. Specifically, the work has solely focused on numeric simulation (modeling) using fundamental calculations and characterization of existing laboratory data. The motivation for the modeling project has been to create a tool for supplementing physical system research. As may be expected, the full system can be quite complex and the optimum configuration choice is not always clear. Using a modeling tool, a system designer can experiment with various configurations and analyze their relative tradeoffs prior to physically building the system of choice. Specific to the air system, various types of compressors and energy recovery devices exist, and with each component comes a unique optimum control scheme for the fuel cell system.

This research, therefore, is designed to address the following motivating questions. First, what model design will realistically characterize the performance of the laboratory-tested air system? And second, what are the relative differences in system performance when the air system configuration is altered? Both of these questions are addressed in this thesis.

Much of the work from this research was published in three independent papers, which are included in this thesis. A few of the research findings are included here.

Section 2.1 highlights an analysis comparing an air system with and without the use of an expander (turbine). It is shown that the use of the expander (turbine) results in an improvement to the system efficiency at peak power levels. However, under normal driving conditions, peak power levels are demanded only a small fraction of the time. Therefore, it becomes less clear as to whether the added complexity and cost of an expander (turbine) would be beneficial. For example, for a fixed fuel cell stack size, the net efficiency is improved by approximately 4 % in the higher power region above 24kW net compared to the system without the expander. However, net efficiency is almost unchanged in the lower power region used most of the time. Alternatively, for a fixed peak power, the stack size can be reduced by about 13% using an expander compared to the fuel cell stack size required in a system without an expander.

Section 2.2 presents findings from a study comparing a low pressure air system to that of a high pressure system. The results of the study demonstrate that equivalent direct hydrogen fuel cell peak net system power values (86kW) can be obtained with both types of air supply configurations but require different stack sizes. For the blower application, the stack size had to be increased by 16.3% (500 vs. 430 cells in this example) for the same peak net power of 86kW.

Finally, Section 2.3 highlights research focused solely on the modeling structure of an air system in the context of the fuel cell engine. It was found that to maximize the performance of a particular fuel cell system configuration, it is useful to have a model that can compare various air supply technologies in the context of the system operation.

## Acknowledgments:

Many people have contributed to this thesis, all of which I am extremely grateful. This project could not have been attempted were it not for the support and patience of the faculty, research staff, and administrative staff at the Institute of Transportation Studies. Specifically, I would like to acknowledge the members of my committee. Professor Myron Hoffman worked most closely with me on the content of this thesis project. I appreciate his patience, clear teaching direction, and friendship. I feel I have grown a great deal under his support. Dr. Robert Moore oversees the research group from which this thesis project is derived. He has been very helpful in structuring the research project, yet allowing (and encouraging) me to follow my own interests and insights. His confidence in me has been enlightening. Professor Daniel Sperling oversees the research institute and provides broad guidance where necessary and for this I am grateful. Finally, I would like to acknowledge the hard work and support I have received from the other research members of the Fuel Cell Vehicle Modeling Program. They have contributed greatly to the models that form the foundation of this thesis project.

## Nomenclature:

$c_p$	= specific heat
$F$	= Faraday's constant
$k_c$	= ratio of specific heats, compressor
$k_t$	= ratio of specific heats, turbine
$I$	= stack total current, amperes
$J$	= stack current density, A/cm <sup>2</sup>
$\dot{m}$	= mass flow rate
$n_{\text{cells}}$	= number of cells in the fuel cell stack
$N$	= shaft speed, in revolutions per minute (RPMs)
$\dot{n}$	= molar flow rate, moles/s
$MW$	= molecular weight, g/mole
$P$	= power, kW
$p$	= pressure, atm
$r_c$	= compressor pressure ratio = $p_{c2} / p_{c1}$
$r_t$	= turbine pressure ratio = $p_{t3} / p_{t4}$
$SR$	= stoichiometric ratio of air: ratio of <b>moles of O<sub>2</sub> in the air per second</b> supplied to fuel cell stack vs. <b>moles of O<sub>2</sub> per second</b> utilized at the corresponding stack power level (or fuel consumption rate)
$T_1$	= ambient and compressor inlet temperature, 25°C or 298K
$T_2$	= compressor exit temperature, Kelvins
$T_3$	= fuel cell stack exit and turbine inlet temperature, Kelvins
$V$	= stack total voltage, volts
$\eta$	= efficiency

## Subscripts:

a	= air
as_motor	= air supply motor characteristic
c	= compressor
cond	= condenser
drag	= H <sub>2</sub> O transported across the membrane
form	= H <sub>2</sub> O formed at from the catalyst reactions
hum	= H <sub>2</sub> O for humidification of air into the fuel cell
rad	= radiator
sh	= shaft
t	= turbine/expander

1 = inlet conditions to the compressor – atmosphere

2 = exit conditions from the compressor and inlet to the fuel cell stack

3 = exit conditions from the fuel cell stack and inlet to the turbine

4 = exit conditions from the turbine - atmosphere

## **Part I: Background**

### ***1.1 Introduction: Context of the air supply in the fuel cell system***

There are a number of reasons why vehicular fuel cell systems are receiving heightened interest. The primary reasons include potential environmental and energy security benefits. When operated on neat hydrogen as the fuel, fuel cell systems release only water and thermal energy in addition to the electricity produced to operate the vehicle drive motors and accessories. When operated on a liquid carbonous fuel, residual emissions of CO, CO<sub>2</sub>, and NO<sub>x</sub> do exist but are potentially low compared to today's vehicles (though this has yet to be proven in use). The concept of energy security is attractive in the sense that use of non-petroleum fuels may reduce a society's dependence on one fuel source and may ultimately lead to renewable fuel sources and/or low full-fuel-cycle emissions. Fuel cell systems also have the potential to be more energy efficient and thus reduce fuel consumption and operating costs.

Recent government regulations as well as dramatically improved system designs (reduced cost and size, improved component integration) are driving the recent fuel cell vehicle R&D. However, much development is still needed. One such area of development is with the air management system.

The operating requirements for the air system in this new application are very demanding. The fundamental purpose of the air compressor (or blower) is to provide oxygen molecules to the fuel cell stack at the cathode catalyst reaction sites. At this location, an electrochemical reduction reaction occurs where hydrogen protons and electrons combine with oxygen molecules to form water. As it is the hydrogen ions that provide the electrical current necessary to drive the vehicle, the oxygen requirements

(and thus compressor loads) are directly dependent on the vehicle propulsion electrical demands. Though the nitrogen in the air is not used in the reaction, the use of an air compression device rather than an oxygen tank is preferred for safety, packaging, and refueling reasons. The nitrogen can hinder the movement of oxygen to the cathode reaction sites. However, the flow of nitrogen in the gas stream can aid in the removal of water from the fuel cell stack.

The amount of air necessary (in terms of mole/s or kg/s) as well as the desired operating air pressures are sufficiently high to demand large electrical parasitic loads at the compressor motor. Because of this, when the fuel cell system is not operating at full power (a majority of the time), the air system output needs to be reduced as well. This now requires a variable flow and pressure air system that results in complex component designs and expensive controllers with a variable speed motor. In an attempt to reduce the compressor parasitic loads, pressurized systems sometimes use expanders (or turbines) to recover energy from the fuel cell stack exhaust gases. This reduces parasitic loads but increases system complexity, packaging concerns, and the matching of air system components.

The magnitude of the air system parasitic loads can be shown in the following diagram for an example direct hydrogen fuel cell system. The difference between the solid and the dashed lines represent the loss in efficiency due to the parasitic loads of the air system.

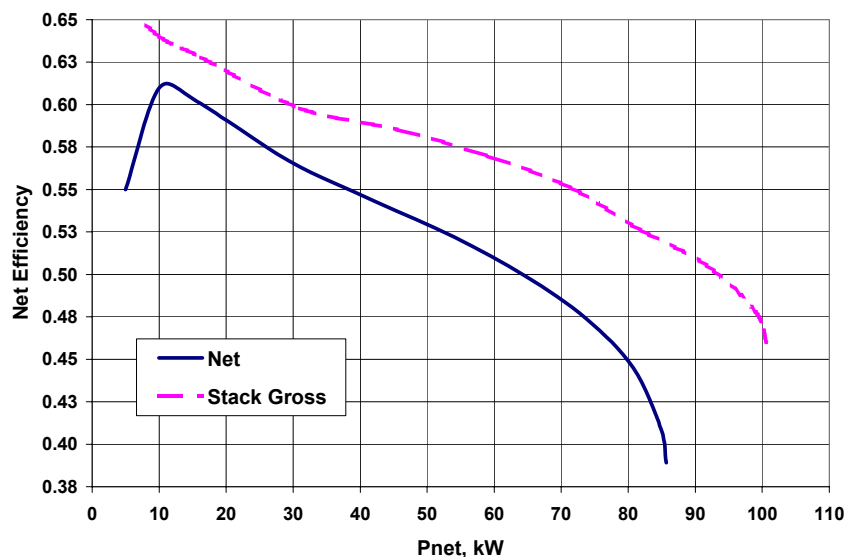


**Figure 1: Example fuel cell stack and net system performance**

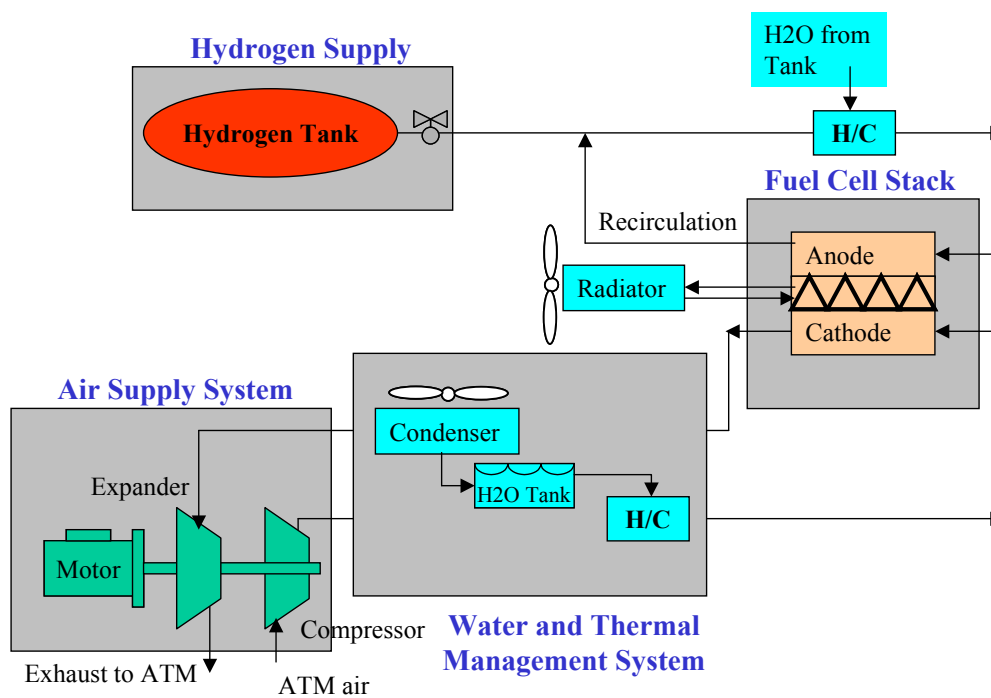
The concept of a variable air flow and pressure control scheme demands a performance optimization between the air system and the particular fuel cell stack chosen. Details of this process can be found in the Appendix (Section 4.1). Additionally, details of the modeling process in general can be found in the Appendix as well.

## ***1.2 Physical system configuration***

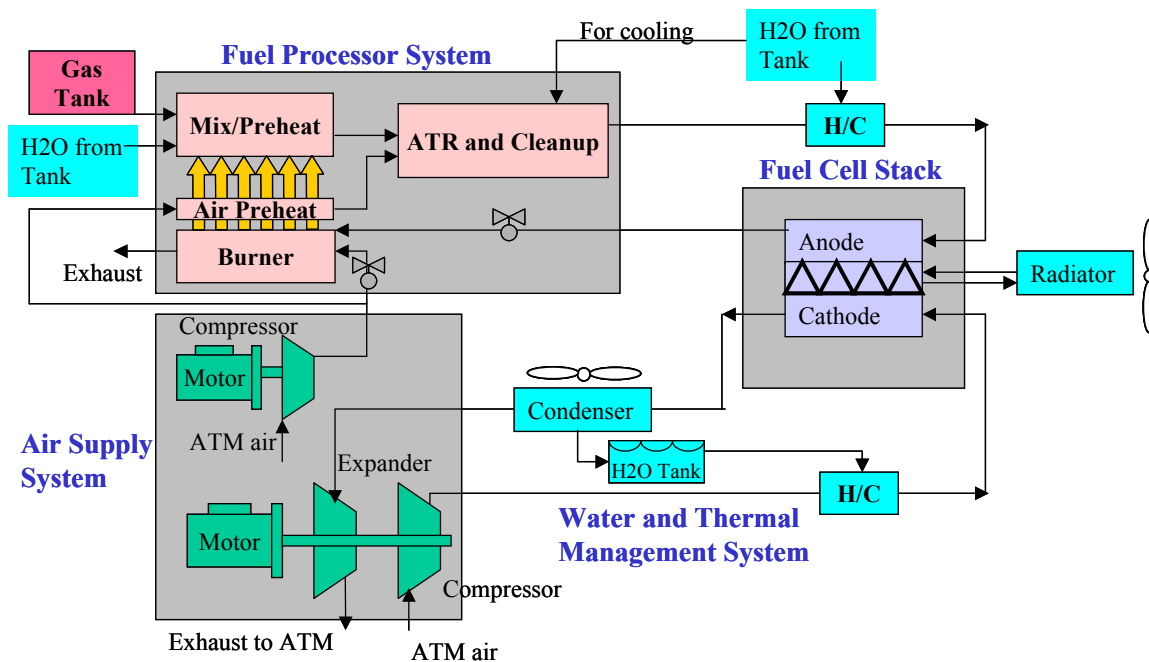
Figure 1 shows two example configurations, one of a Direct Hydrogen Fuel Cell System (DHFC) and the other an Indirect Hydrocarbon Fuel Cell System (IHFC). There are a number of different component configurations possible, the arrangement shown is simply one such configuration. Additionally, other fundamentally different fuel-dependent designs are under consideration, namely the Indirect Methanol and the Direct Methanol Fuel Cell Systems (IMFC and DMFC).

All of the system configurations require an air management sub-system, however. For the IHFC and the DHFC in the figure, the air system is essentially the same, where

the air system/cathode loop is independent from the fuel/anode loop (This is contrary to some developments, for example, that combine the anode and cathode exhaust streams and heat the combined stream in a burner.) The only major difference between the two systems shown (in terms of the air management) is that the IHFC requires a second means of air supply for use in the fuel processing sub-system. This can be accomplished with a second, independent compressor, as shown in Figure 2.



**Direct Hydrogen Fuel Cell System**



### Indirect Hydrocarbon Fuel Cell System

**Figure 2: Example system configurations**

In addition to the interaction with the fuel cell stack, the air system also interacts with water and thermal management components. In the systems shown, the air entering the fuel cell stack (exiting the compressor) needs to be humidified such that water can be transported to the fuel cell stack membrane. Though water is generated at the cathode reaction sites, the fuel cell membrane may not be properly humidified at the inlet locations. The humidification also acts to cool the heated air, which may be necessary if the air is sufficiently hotter than the desired stack temperature (normally 80°C for PEM fuel cell stacks). Following the stack reactions, it is necessary to recover liquid water from the stack exhaust stream. This stream consists of excess oxygen, the nitrogen, and water liquid and vapor. If the amount of liquid water is not sufficient, a condenser is necessary. This condenser may be placed prior to (as shown in Figure 2) or following an expander (turbine), with tradeoffs in both scenarios.

The compressor/expander arrangement shown in Figure 2 is typical for this application. A variable speed motor operating with a current draw from the fuel cell stack controls the compressor. Control of the back-pressure acting on the compressor as well as the motor shaft speed allow for the control of the desired air flow into the fuel cell stack. Following the stack and water auxiliaries, the cathode exhaust enters the expander (turbine) where shaft power is recovered as the gas stream expands and cools. If the components are matched properly, the expander may act as the back-pressure device for the air supply loop. Otherwise, a valve is required.

The flow composition entering the expander will vary depending on the configuration choice. For example, the placement of the condenser prior to the expander (as shown) ensures that the gas stream will be at a lower mass flow rate, temperature and pressure compared to that of the fuel cell stack exit. This reduces the potential energy recovery in the expander but allows the condenser to operate at a relatively high pressure. In other configurations where the cathode exhaust may be heated by the burner thermal energy, the temperature of the gas entering the expander will be higher than the stack exhaust, increasing the potential for energy recovery.

### ***1.3 Modeling the Air Supply System Components***

#### **Compressor Relationships:**

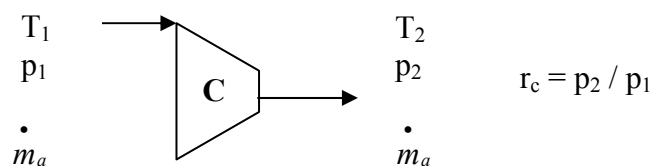


**Figure 3: Compressor parameters**

The theoretical maximum power used for purposes of efficiency calculations is the isentropic power of compression and is defined as follows:

$$P_{c\_isen} = \dot{m}_a c_{pc} T_1 \left( r_c^{\frac{kc-1}{kc}} - 1 \right) \quad (1)$$

In reality, irreversibilities occur increasing the actual power necessary for compression. The thermodynamic, non-isentropic power of compression, not including mechanical friction irreversibilities is defined in Equation 2. Here, if the output temperature ( $T_2$ ) or  $\eta_{c\_isen}$  is known,  $P_{c\_thermo}$  can be determined.

$$P_{c\_thermo} = \dot{m}_a c_{pc} (T_2 - T_1) = \frac{P_{c\_isen}}{\eta_{c\_isen}} \quad (2)$$

where

$$\eta_{c\_isen} = \frac{P_{c\_isen}}{P_{c\_thermo}} \quad (3)$$

In mechanical systems, additional energy losses arise from the friction of the moving components. If this mechanical efficiency is taken into consideration, the input energy necessary at the compressor shaft can be determined.

$$P_{c\_shaft} = \frac{P_{c\_thermo}}{\eta_{c\_mechanical}} \quad (4)$$

### Expander Relationships:

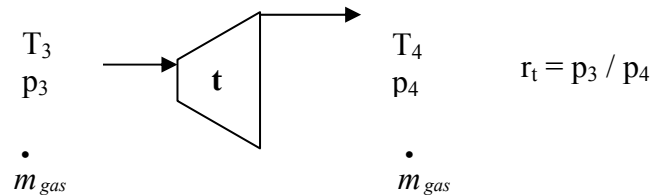


**Figure 4: Expander (t) parameters**

The relationships for the expander follow the same logic as that of the compressor. The isentropic and thermodynamic powers of expansion are as follows:

$$P_{t\_isen} = \dot{m}_{gas} c_{pt} T_3 \left( 1 - r_t^{\frac{1-k_t}{k_t}} \right) \quad (5)$$

$$P_{t\_thermo} = \dot{m}_{gas} c_{pt} (T_3 - T_4) = \eta_{t\_isen} * P_{t\_isen} \quad (6)$$

where

$$\eta_{t\_isen} = \frac{P_{t\_thermo}}{P_{t\_isen}} \quad (7)$$

Note that the mass flow is not that of pure air, but rather the residual gas stream from the exit of the fuel cell stack. The resulting recovered shaft power is as follows:

$$P_{t\_shaft} = \frac{P_{t\_thermo}}{\eta_{t\_mechanical}} \quad (8)$$

The residual gas stream is an oxygen-depleted air along with water vapor. The presence of water in the exhaust stream can significantly impact the performance of the expander. If the mass flow of water vapor is large, additional expander energy can be recovered. Additionally, as the gas stream expands and cools, water vapor may condense in the expander therefore reducing system condenser parasitic loads.

### **Combined Relationships:**

For the purposes of determining the electric motor power for the air system, the combined characteristics need to be determined.

$$P_{motor\_mech} = P_{c\_shaft} - P_{t\_shaft} \quad (9)$$

$$P_{motor\_elec} = \frac{P_{motor\_mech}}{\eta_{motor}} = V_{stack} * I_{as\_elec} \quad (10)$$

The electric motor for the air system operates at the same voltage as the fuel cell stack. A current draw is established to operate the motor and is subtracted from the total current of the stack.

### **Fuel Cell Stack Relationships:**

The amount of air necessary for the fuel cell cathode reactions to occur can be defined as in Equation 11. Notice that this shows a relationship between utilized air flow rate and the stack total current (the factor of 4.76 represents the number of moles of air relative to the number of moles of oxygen in that quantity of air).

$$\dot{m}_{a\_utilized} = \frac{I_{stack} 4.76 MW_{air} (n\_cells)}{4F} \quad (11)$$

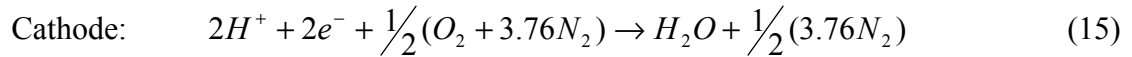
However, in dynamic fuel cell systems, excess air is desired to ensure that sufficient air is present when necessary and to aid in the removal of the water present in the cathode channels. The actual amount of air demanded from the air compressor is defined in Equation 12 where the Stoichiometric Ratio is applied.

$$\dot{m}_a = SR \dot{m}_{a\_utilized} \quad (12)$$

To complete the description and determine the corresponding flow of fuel, the following equation shows the relationship between the fuel flow and the same total stack current used in Equation 11.

$$I_{stack} = \frac{\dot{m}_{h2\_utilized} 2F}{(n\_cells) MW_{h2}} \quad (13)$$

For completeness, Equations 14 and 15 show the electrochemical reactions that occur at the fuel cell stack electrodes.



#### ***1.4 Mathematical modeling: A summary***

A model is needed with a defined set of performance criteria and data input format, one that can accommodate multiple air supply configurations, and one that realistically and accurately simulates the air supply operation and its effect on the system power and efficiency.

This section describes the approach used to model the fuel cell system air supply. Note that much of the information is *specific to centrifugal compressor technology* (a.k.a. turbocompressor), however, the final model incorporates data for multiple compressor types.

#### **Performance Maps**

The data input format is based on compressor performance maps. An example of one of these performance maps is shown in Figure 5, a map that is used for a centrifugal compressor technology [Ref. 11, AlliedSignal]. Figure 6 provides a map of corrected  $P_{\text{shaft}}$  vs. corrected speed [Ref. 11, AlliedSignal].

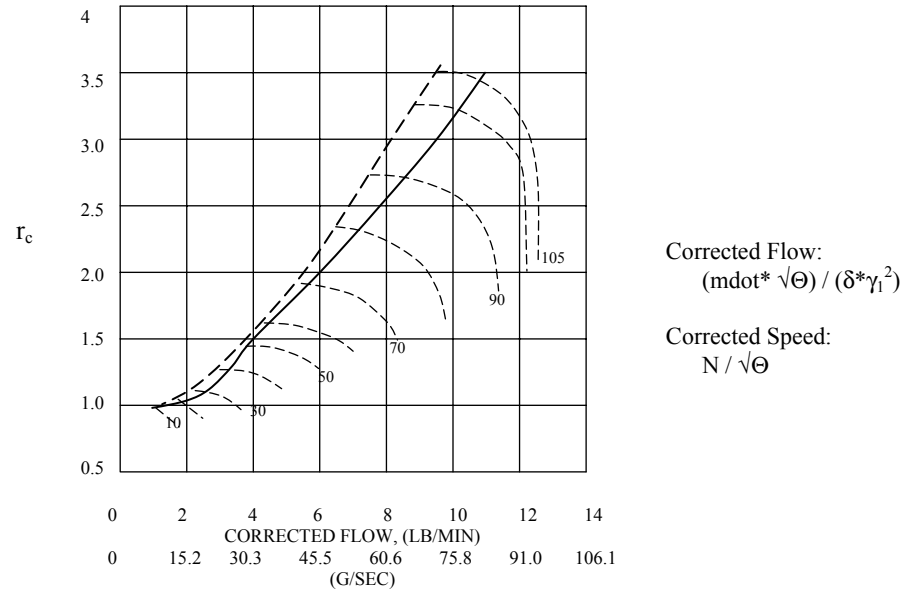


**Figure 5: Pressure Ratio vs. Corrected Mass Flow [Ref.3]**

where the curved dashed lines that progress from upper-left to lower-right represent constant corrected speed lines (thousands of RPMs: kRPM), the single dashed line represents the surge line, and the single solid line represents the operating line

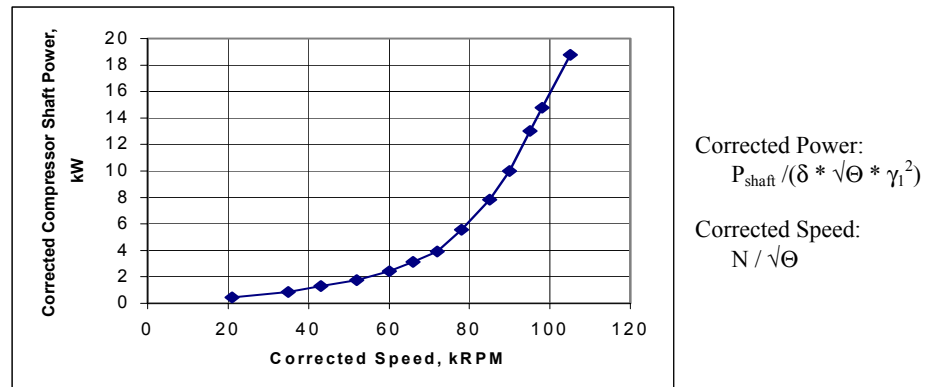


**Figure 6: Shaft Power vs. Mass Flow along the operating line [Ref.3]**

The corrected variables used in Figures 5 and 6 are defined as:

$$\Theta = T (K) / 298 K$$

$$\delta = p (atm) / 1.0 atm, \quad p = \text{pressure}$$

These maps can incorporate a number of descriptive features. First, the Figure 5 map defines the relationship between pressure ratio, the mass flow of air, and corrected shaft speed. Second, Figure 6 specifies the corresponding corrected motor shaft mechanical power for each  $r_c$ /mass-flow/shaft-speed combination on the operating line. Third, they can show the limiting ranges of  $r_c$  and mass flow attainable with the specific compressor technology.

The key modeling problem is how to incorporate the data on performance maps into the air supply model in the fuel cell system code. This is discussed below.

### **The Air Supply Model**

The model has the flexibility to simulate various air supply technologies. This is very useful in determining which technology is best suited for a given fuel cell system and vehicle configuration. Currently, fuel cell system developers are working with a number of different technologies that include reciprocating piston, twin screw, scroll, and turbo compressor designs. The model includes a section for each type of air supply technology. For accurate technology comparison and model consistency, a common set of input and output parameters are utilized. This also allows for incorporation into the fuel cell system model in a way that is consistent for all the air supply technologies.

For an individual simulation, one type of technology is chosen. Once the ambient conditions for the specific computer simulation run are defined, the air supply model uses this information along with the required air mass flow rate ( $\dot{m}$ ) and pressure ratio ( $r_c$ ) as inputs to "look-up tables". The output results are in the form of the actual required  $P_{\text{shaft}}$  and  $N$  (shaft RPM). With this information, an electric motor map is utilized to

determine the consumed electrical power for compression. The consumed power is then used for calculating the fuel cell system *net* power output and *net* efficiency.

The model can also be used to compare various compressor technologies. Several compressor features are important when comparing the various technologies. First, the maximum shaft speed and power limits of the particular technology can be analyzed to determine if the air supply is scaled properly for the application. Second, the air supply technology can be chosen such that it operates near its most efficient performance point over a large percentage of the specific driving cycle (corresponding to fuel cell system power demands). Third, physical size and weight can be considered when packaging the air supply in the vehicle application, though this is not explicitly included in the model.

Once the required net shaft power ( $P_{c\_shaft} - P_{t\_shaft}$ ) is known, the corresponding electric motor power required is evaluated (Equations 9 and 10). Performance maps are utilized to calculate the shaft speed (based on the pressure ratio and the mass flow rate required). With the speed and the shaft power, the mechanical torque is calculated. The shaft speed and torque are then used with a motor performance map to determine the motor efficiency for the given performance point. The electric motor power required is then equal to the motor shaft power divided by the motor efficiency.

### **The Optimization between the Air System and the Fuel Cell Stack**

An independent optimization model has been created to determine the operating scheme of the air system in the context of the fuel cell stack's cathode characteristics. Using the fuel cell current density as the independent variable, the optimization code "searches" for the  $p_{oxygen}$  (partial pressure of oxygen at the catalyst reaction sites) and air mass flow rate that will generate the maximum net electric power for each value of the

current density. In doing so, cell voltage vs. current density characteristics are taken into account, and total air pressure is directly calculated from the partial pressure of oxygen based on the cathode physical characteristics. The defined net electric power is simply the resulting stack gross electric power minus the resulting air system electric motor power necessary (determined from the air system model). The end result is a performance map of the fuel cell stack / air system combination that provides net system efficiency and net system power for each value of current density.

### ***1.5 Technology options and applicable system configurations***

#### **Current Air Supply Developers**

The following is a brief summary of the types of compressors currently under development for fuel cell applications. Several of the compressor developers are under contract with the US Department of Energy, and a few of the compressor types have been placed in actual fuel cell vehicle prototypes

1. ***AlliedSignal Aerospace:*** The design is a centrifugal turbocompressor similar to that used for combustion engine turbocharging. The primary difference is that a supplemental electric motor is needed to provide the compression energy not recovered from the turbine. This technology shows promise considering it is well developed. However, though the compressor can obtain the desired pressure ranges (up to 3.2 pressure ratios), it is difficult to design a single compressor that can provide the full range of mass flow demanded. Additional development is needed in the area of very high-speed motors for this compressor type since the motor can be expensive. The company currently has a contract with the US DOE for vehicular fuel cell applications.

2. **Arthur D. Little:** The design under development is an orbiting scroll technology (positive displacement) similar to that used in many stationary refrigeration and vehicular air conditioning applications. The compressor has the ability to provide a continuous stream of air (no pulsation) but due to built in clearances in the device, higher pressure operation (above 3.0 pressure ratios) is difficult. The company currently has a contract with the US DOE for vehicular fuel cell applications.
3. **Meruit Inc.:** Similar to the AlliedSignal contract, the design concept is a turbocompressor. Meruit's contract includes the development of advanced air bearings for use in the turbocompressor. The company currently has a contract with the US DOE for vehicular fuel cell applications.
4. **OPCON:** This European company produces a positive displacement screw compressor technology commonly used for combustion engine supercharging applications. The technology will compress air to the desired pressure ranges (up to 3.2 pressure ratios), and can provide the desired mass flow (up to approximately 80 g/s). However, the efficiency of the technology is not as good in the lower pressure – flow regions, and significant airborne noise is characteristic of this compressor type. This technology is common initial choice for vehicle prototypes considering it can be obtained ‘off-the-shelf’ and can operate well in the low pressure and mass flow regions (below 2.0 pressure ratios and 30 g/s).
5. **Vairex Corp.:** The design is a "variable geometry" positive displacement piston compressor. By varying either the piston displacement or the exhaust valve

opening, air mass flow and pressure ratio can be controlled independently. This attribute is not possible with the other compressor technologies without the use of additional valving. Though the concept appears to be promising, it is not a well-developed technology, and appears to be complex. The company currently has a contract with the US DOE for vehicular fuel cell applications.

6. ***Wankel Compressor:*** An additional type of air compressor that may be developed for this application is a device similar to that of the Wankel rotary engine. This technology was not investigated through the scope of this research.

The above compressors are in various stages of development. However, there is optimism that some of the designs will be commercially available in the near future.

## **Part II: Model Studies and Simulations**

### ***2.1 Use of an expander (turbine)***

As shown previously, an energy recovery device (expander or turbine) is commonly considered in the system design. The cost, complexity, and packaging of the extra component may be worthwhile if sufficient shaft energy can be recovered to reduce the input energy demands of the compressor. The following section summarizes a modeling study of the use of an expander in the system context. The full research paper can be found in the Appendix, Section 4.3.1.

#### **Abstract**

This paper compares the performance of various air supply configurations in an automotive PEM fuel cell system. An air supply configuration that uses only a compressor will be compared to a system that incorporates an expander (turbine) for energy recovery in addition to the compressor. It is shown that the use of the expander (turbine) results in an improvement to the system efficiency at peak power levels. However, under normal driving conditions, peak power levels are demanded only a small fraction of the time. Therefore, it becomes less clear as to whether the added complexity and cost of a turbine would be beneficial.

The following two figures show the key results.

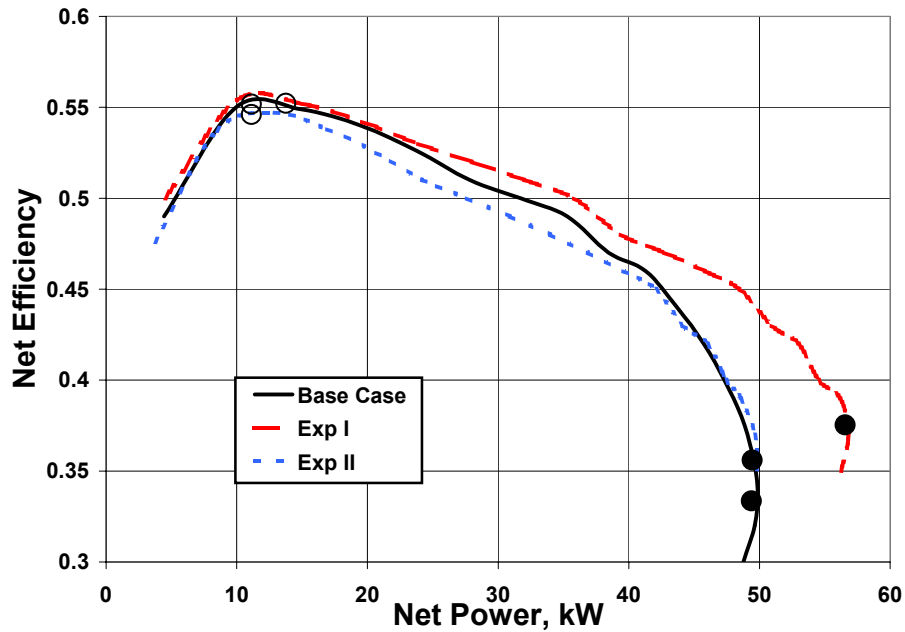


Figure 7: Net Efficiency vs. Net Power

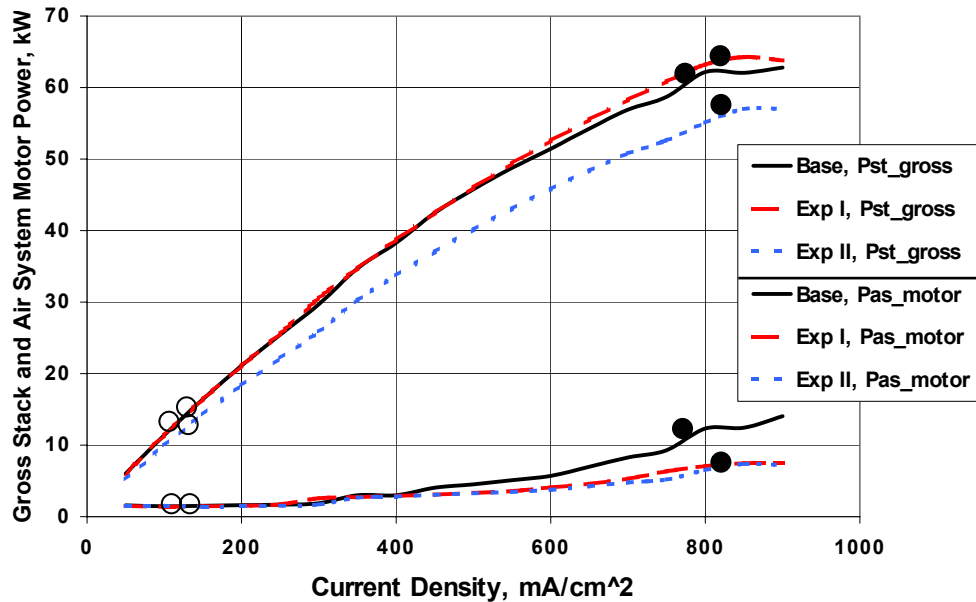


Figure 8: Electric Power vs. Current Density

Key: ● = 100% and ○ = 25% of peak net system power

## Conclusions

The following results and trends can be deduced from Figures 7 and 8:

- For the turbine configuration with the same size stack relative to Base Case (Exp I):

- The net efficiency is noticeably improved in the higher power region above 24kW net. Specifically, the net efficiency is improved by up to 4 percentage points at 45kWnet. However, net efficiency is almost unchanged in the lower power region.
- Peak net power capability is increased by 14%
- For the turbine configuration with reduced stack size relative to Base Case (Exp II):
  - The stack size is reduced by 13% while the peak net power capability is maintained
  - Noticeable reductions in net efficiency are apparent for much of the net power range. Specifically, between 15 and 35kW net power, the net efficiency for Exp II is reduced by 1 to 1.5 percentage points. Unfortunately, the lower power region is where the vehicle operates most of the time
  - Net costs would improve if the incremental cost reduction of the stack outweighs the increased cost of the turbine. Results from an ArthurDLittle cost study indicate that the incremental cost of the stack size far outweighs the cost of the air system components (Ref. 32).
- A significant portion of the cathode exhaust flow is water vapor that can be useful in the turbine's energy recovery. For the design point example presented, 60% of the total cathode water mass flow was water vapor. This is equal to approximately 19% of the total cathode exhaust gas mass flow ( $N_2$ ,  $O_2$ , and  $H_2O_{vap}$  combined). Exactly how much the given water vapor could improve turbine performance (calculated for dry air in this study) is a complex function of the condensation and heat release in the turbine. This will be the subject of future research.

- With the use of a turbine, air system control methods become more complex. The fuel cell stack pressure and the air mass flow would be controlled by varying the compressor/turbine common shaft speed *and* by varying the geometry of the turbine (variable vane positions). These two parameters can be used to control the backpressure from the turbine (and thus fuel cell system operating pressure) as well as the mass flow. In a system without a turbine, backpressure is controlled with a simple flow valve at the exit of the fuel cell stack (or possibly at the condenser exit). This valve may be necessary in a system with a turbine that does not incorporate variable geometry control.
- By adding a turbine, system complexity is increased. Specifically, the addition of an extra component alters volume (packaging) considerations. The reduction in stack and condenser size may offset the turbine volume but the packaging would still be different (in terms of shapes and component location).

In conclusion, it has been shown that the use of a turbine has its benefits and drawbacks. A developer's configuration of choice will depend on the magnitude of the tradeoffs between system costs, weight, volume and net performance.

## ***2.2 High pressure vs. low pressure system operation***

Considering the parasitic loads of the compressor can be significant for operation with pressurized air, several developers continue to experiment with near-ambient pressure operation. The following section summarizes a comparison of the system performance and physical characteristics using both pressure schemes. The complete paper can be found in the Appendix, Section 4.3.2.

## **Abstract**

This paper compares the merits of operating a direct-hydrogen fuel cell (DHFC) system using a high-pressure air supply (compressor) versus one using a low-pressure air supply (blower). Overall, for the system modeled, it is shown that there is no inherent performance advantage for either mode of operation at the DHFC stack level. However, in practical applications, as will be shown in this paper, a systems analysis (stack and air supply) of power and efficiency needs to be performed.

Equivalent PEM DHFC stack peak power values can be obtained using both high-pressure and low-pressure air supply systems. For each air supply configuration, air mass flow and pressure operating conditions can be found that result in an equal value of the oxygen partial pressure at the cathode catalyst layer surface.

However, at the system level, the required air supply power needed to achieve the same DHFC stack performance values can be drastically different for high and low pressure operation. In order to compare the two systems, an optimal air supply control strategy is first developed to obtain the desired stack operating conditions with minimal parasitic loads based on each air supply configuration. Second, the resulting air supply parasitic loads are compared directly between the two configurations – both comparisons are set in the context of the system performance. In other words, the systems are sized such that the peak net power values are equal while the stack gross power may be different.

The results of the study demonstrate the well-known fact that equivalent DHFC peak net system power values (86kW) can be obtained with both types of air supply configurations but require different stack sizes. For the blower application, the stack size

had to be increased by 16.3% (500 vs. 430 cells in this example) for a peak net power of 86kW. Differences are also apparent with the WTM sub-system. Quantitative results will be presented for both the high pressure and the low pressure applications.

**Table 1: System Power and Efficiency**

Parameter	Compressor	Blower
P <sub>net</sub> , kW	85.7 (18.0)	86.6 (18.4)
P <sub>as_motor</sub> , kW	14.2 (0.8)	2.9 (0.4)
Ratio P <sub>as_motor</sub> /P <sub>stack</sub>	0.14 (0.04)	0.03 (0.02)
Efficiency <sub>stack</sub> (LHV) %	45.7 (62.3)	42.9 (62.4)
Efficiency <sub>net</sub> , %	38.9 (59.6)	41.1 (61.0)

*Values in ( ) are for part load performance, approximately 21% of peak net power*

**Table 2: Conditions at stack exit – Comparison at peak load condition**

Parameter	Compressor	Blower
P <sub>net</sub> , kW	85.7	86.6
P <sub>stack</sub> , kW	100.8	90.4
Current density, mA/cm <sup>2</sup>	850	700
Total current, A	417	343
r <sub>c</sub> , at the exit of the stack	1.8	1.01
Air stoichiometric ratio	1.5	1.3
• m <sub>h2o-form</sub> , g/s	19.4	16.0
• m <sub>h2o-drag</sub> , g/s	4.0	3.2
• m <sub>h2o-hum</sub> , g/s	1.1	0.8
• m <sub>h2o-total</sub> , g/s vapor and liquid	24.5	20.0
% of exit water mass flow in vapor form	88 %	100 %

\* Note: Assumes dry air into compressor inlet and a stack operating temperature of 80°C

## Conclusions

The following conclusions can be made from these specific simulations:

1. The same peak P<sub>net</sub> can be achieved with both a blower (low pressure) and a compressor (high pressure), but the required fuel cell stack sizes are different. For the same peak P<sub>net</sub> of 86kW, 16.3% more operating PEM cells were needed in the stack for the blower application (500 vs. 430 cells with a constant active area of 490cm<sup>2</sup>).

2. The blower system was able to obtain the same net power by operating just above ambient pressure at the stack and providing sufficiently higher air mass flow rates compared to that of the compressor for much of the  $P_{\text{net}}$  range.
3. The parasitic loads for the blower are significantly less than that of the compressor at the high  $P_{\text{net}}$  region. The ratio of  $P_{\text{as\_motor}}/P_{\text{stack}}$  was 14.1% for the compressor vs. 3.2% for the blower at a peak  $P_{\text{net}}$  of 86kW (though these occur at different  $P_{\text{stack}}$  values).
4. Overall, the net system efficiencies over the  $P_{\text{net}}$  range were very similar for both the blower and the compressor. However, the blower system did maintain a net efficiency 1.5 – 2.0 percentage points higher than the compressor system over most of the net power range.
5. High pressure application results would differ if an expander were to be included.  $P_{\text{net}}$  would be achieved at reduced  $P_{\text{stack}}$  powers and thus different air pressure and mass flow schemes. Stack size would be further reduced, potentially increasing overall power density and reducing costs. Net system efficiency *may* improve as well.

### ***2.3 Corrections for ambient conditions and geometry***

The following section summarizes the complexities of modeling an air system, and discusses concepts of correcting performance data for varying ambient conditions and geometry. The full research paper can be found in the Appendix, Section 4.3.3.

## Abstract

This paper addresses the critical need to incorporate realistic models of the air supply sub-system in fuel cell system performance analysis. The paper first presents the dominant performance issues involved with the air supply operation in the fuel cell system. The report then goes on to propose a methodology for an air supply model that addresses many of the performance issues. Most importantly, a model is needed with a defined set of performance criteria and data input format, one that can accommodate multiple air supply configurations, and one that realistically and accurately simulates the air supply operation and its effect on the system power and efficiency. The paper concludes that it is possible to compare alternative air supply components under the constraint of maximizing the instantaneous net fuel cell system efficiency for a dynamic vehicle driving cycle under various ambient conditions.

## System Context:

The pressurized airflow is a result of a compression process that requires input energy. The electrical power required to compress the air must be subtracted from the "gross power" of the fuel cell stack. The fuel cell stack gross power minus the power of the air supply is thus titled the "net system power" (currently, this net power does not include recovered energy through the use of an expander unit). This implies the need to compare various air supply technologies. By maintaining the same fuel cell stack characteristics, the system performance results from the use of varying air supply technologies can be studied. The two dominant performance characteristics are the net system power and the net system efficiency.

$$P_{\text{net\_system}} = P_{\text{gross\_stack}} - P_{\text{comp}} \quad [16]$$

$$\eta_{\text{net\_system}} = P_{\text{net\_system}} / [(LHV \text{ of } H_2) * \dot{m}_{H_2}] \quad [17]$$

where  $P$  represents "power" and  $LHV$  is the lower heating value per unit mass of fuel

### Corrected Data and Performance Maps:

In order to create a model that is flexible enough to simulate various ambient performance conditions, it is necessary to use "corrected variables". The following is an example of how one might correct the data. Note that this is an example for a *centrifugal air compressor* and the format for the corrected data will vary depending on the technology used.

The corrected variables used are:

$$\Theta = T \text{ (K)} / 298 \text{ K}$$

$$\delta = p \text{ (atm)} / 1.0 \text{ atm, } p = \text{pressure}$$

$G_1$  = characteristic dimension used for physical scaling

(where  $G$  can be length, area, or volume)

$G_2$  = additional characteristic dimension used for

physical scaling (when multiple scalars are needed)

$$\gamma_1 = G_1 / G_{\text{ref1}}$$

$$\gamma_2 = G_2 / G_{\text{ref2}}$$

The format for correcting the performance parameters is as follows:

$$\text{Compressor pressure ratio: } p_{\text{out}} / p_{\text{in}} = r_c \quad [18]$$

$$\text{Corrected mass flow: } (\dot{m} * \sqrt{\Theta}) / (\delta * \gamma_1^2) \quad [19]$$

$$\text{Corrected shaft speed: } N / \sqrt{\Theta} \quad [20]$$

$$\text{Corrected shaft power: } P_{\text{shaft}} / (\delta * \sqrt{\Theta} * \gamma_1^2) \quad [21]$$

The corrected variables may take the following **general form**:

$$\text{Compressor pressure ratio: } p_{\text{out}} / p_{\text{in}} = r_c \quad [22]$$

$$\text{Corrected mass flow: } \dot{m} \cdot \delta^{X1} \cdot \Theta^{Y1} \cdot \gamma_1^{Z1} \cdot \gamma_2^{V1} \quad [23]$$

$$\text{maximum allowable: } \dot{m}_{\text{max}}(N_{\text{max}}) \cdot \delta^{X2} \cdot \Theta^{Y2} \cdot \gamma_1^{Z2} \cdot \gamma_2^{V2}$$

$$\text{Corrected shaft speed: } N \cdot \delta^{X3} \cdot \Theta^{Y3} \cdot \gamma_1^{Z3} \cdot \gamma_2^{V3} \quad [24]$$

$$\text{maximum allowable: } N_{\text{max}} \cdot \delta^{X4} \cdot \Theta^{Y4} \cdot \gamma_1^{Z4} \cdot \gamma_2^{V4}$$

$$\text{Corrected shaft power: } P_{\text{shaft}} \cdot \delta^{X5} \cdot \Theta^{Y5} \cdot \gamma_1^{Z5} \cdot \gamma_2^{V5} \quad [25]$$

where the exponents have to fit the data supplied by the compressor developers, and will be unique for each compressor type.

For an individual simulation, one type of technology is chosen. Once the ambient conditions for the specific computer simulation run are defined, the air supply model will use this information along with the required  $\dot{m}$  as inputs to "look-up tables" (which includes the compressor performance maps). The output results should be the actual required  $P_{\text{shaft}}$ ,  $N$ , and  $r_c$ . With this information, an electric motor map is utilized to determine the consumed electrical power for compression. The consumed power is then used for calculating the fuel cell system *net* power and *net* efficiency.

### Turbocompressor Example

**Table 3: Input values and exponents**

	<b>Scenario 1</b>	<b>Scenario 2</b>
	<b>STP</b>	<b>Denver,CO</b>
<b>Ambient:</b>		
$T_{\text{amb}}$	298 K(25C)	308 K(35C)
$P_{\text{r\_amb}}$	1 atm	0.8 atm
$G_1 = G_{\text{ref1}}$	1	1
$G_2 = G_{\text{ref2}}$	1	1
<b>Exponents:</b>		
$x1, y1, z1, v1$	-1, 0.5, -2, 0	-1, 0.5, -2, 0
$x2, y2, z2, v2$	-1, 0.5, -2, 0	-1, 0.5, -2, 0
$x3, y3, z3, v3$	0, -0.5, 0, 0	0, -0.5, 0, 0
$x4, y4, z4, v4$	0, -0.5, 0, 0	0, -0.5, 0, 0
$x5, y5, z5, v5$	-1, -0.5, -2, 0	-1, -0.5, -2, 0

<b><math>\dot{m}</math> requested (g/s), actual:</b>		
$\dot{m}_{1}$	10	10
$\dot{m}_{2}$	25	25
$\dot{m}_{3}$	40	40
$\dot{m}_{4}$	55	55
$\dot{m}_{\max}$	78.3	60.1

The exponents are based on actual lab data and utilize the format shown in Equations 19, 20, and 21.  $\dot{m}_{\max}$  is based on an assumed  $N_{\max} = 105\text{kRPM}$ .

**Table 4: Output results (compressor only)**

<b>Scenario 1</b>				
	<b>P<sub>shaft</sub></b>	<b>N</b>		
	<b>(kW)</b>	<b>(kRPM)</b>	<b>PR</b>	
$\dot{m}_{1}$	0.23	20.3	1.05	
$\dot{m}_{2}$	1.266	45.8	1.29	
$\dot{m}_{3}$	3.451	68.6	1.85	
$\dot{m}_{4}$	7.178	84.7	2.4	
<b>Scenario 2</b>				
	<b>P<sub>shaft</sub></b>	<b>N</b>		<b>Increase</b>
	<b>(kW)</b>	<b>(kRPM)</b>	<b>PR</b>	<b>in P<sub>shaft</sub></b>
$\dot{m}_{1}$	0.314	21.7	1.09	36.5%
$\dot{m}_{2}$	1.74	58.9	1.55	37.4%
$\dot{m}_{3}$	4.551	82.7	2.19	31.9%
$\dot{m}_{4}$	11.06	98.2	3	54.1%

*Note 1: The above data was derived using the operating line on a performance map.*

*Note 2: The shaft power and speed above are the actual, uncorrected data.*

## Conclusion

Overall, it has been pointed out that a realistic air supply model is necessary for use in fuel cell system development. There are two prominent reasons for this. First, to accurately analyze fuel cell system results, the power consumption of the air supply needs to be subtracted from the gross output power from the fuel cell stack. Second, to maximize the performance of a particular FCV system configuration, it will be necessary to compare various air supply technologies in the system model.

With that as motivation, this paper has provided a methodology for creating a flexible and realistic air supply model. The model utilizes air supply performance maps incorporating pressure ratio, corrected air mass flow rate, operating efficiency, corrected motor shaft speed, and corrected motor shaft power. These are incorporated into the simulation model as table look-ups.

As a final note, it is important to reiterate that this research needs air supply developer feedback to determine if this is the best method for incorporating their particular compressor/expander performance characteristics into the simulation.

## ***2.4 Air system transients***

### **Background**

In general, there are two primary system characteristics that may result in a transient delay from the time the compressor motor is supplied with sufficient electrical power (relative to a demanded air pressure and air mass flow) to the time that the air pressure and flow reach the fuel cell stack cathode reaction sites. First, there is a time associated with changing the state of the air in the entire physical volume of pipes and cathode channels. This may be thought of as “charging” the system. The time delay will be relatively larger if the system needs to be changed from a low pressure (i.e. 1.2 atms) to a higher pressure (i.e. 3.0 atms). Additionally, the time delay is dependent on the size of the physical volume. For example, if the compressor is placed at the opposite end of the vehicle from the fuel cell stack, the time delay will be relatively larger.

The second time delay is associated with the inertia of the compressor shaft movement. Specifically, an increase (from a steady state operation) in the rotational

speed of a spinning object cannot occur instantaneously. This rotating mass may include the compressor rotors or pistons.

To address the first transient effect, that of the physical volume constraints, this research focused on two activities. First, an extensive literature search was conducted investigating pipe dynamics and step responses to input gas state changes. Fundamental textbooks and research papers from other applications were studied. Second, a model was created to test the volume effects using the Matlab Simulink code. The model used simple control logic of feedback loops, sending information to the “upstream” control volumes regarding the downstream gas state conditions. An investigation of the inertia effects and a possible time delay was not pursued due to research time constraints.

### **Research Findings**

The literature search only revealed a few papers that provided quantitative information useful to our application. An ASME paper written in 1971 (Ref. 24, Kantola) showed that the time constants associated with pressurizing the system volume with the desired mass flow are very small. Experimental results in this paper show time constants of less than 0.1 seconds associated with pressurizing a small diameter (0.19 inches) yet long pipe (250 feet). The simple control model created revealed time constants on the same order of magnitude.

Extensive, detailed modeling was not pursued at this point because of the magnitude of the time constants. However, this could be an area of further research. Specifically, shaft inertia effects on the compressor should be investigated.

## **Part III: Closing remarks**

### ***3.1 Conclusion***

The focus of this research has been on the air management system of the fuel cell powertrain in the vehicular application. Specifically, the work has solely focused on numeric simulation (modeling) using fundamental calculations and characterization of existing laboratory data. The motivation for the modeling project has been to create a tool for supplementing physical system research.

Two motivating questions were posed at the beginning of the research:

- First, what model design will realistically characterize the performance of the laboratory-tested air system?
- And second, what are the relative differences in system performance when the air system configuration is altered? Both of these questions are addressed in this thesis.

This thesis has addressed both questions. Specifically, a model was described that incorporated both performance data input files and first principle relationships. Next, three published studies have been summarized, each emphasizing a different aspect of the air management and the relevant system context. Overall, a single conclusion from this research would be that the control of the air management system needs to be carefully considered in the context of the full fuel cell system. The stack and the water/thermal management components are largely dependent on the air stream conditions.

### ***3.2 Future research***

This work has attempted to highlight the important performance issues in a rapidly changing industrial development. Further analysis and development on full air management systems and controls could focus on the following items:

- Proper balancing and control between the expander and the compressor, mechanically
- Providing air to the fuel processor systems (in addition to the fuel cell stack). This introduces an additional control balance
- Airborne and structure borne noise resonating from the air compressor
- Where cathode humidification is necessary, water injection into the compressor during the compression process could reduce air system parasitic loads

## Part IV: APPENDIX

### 4.1 References

#### Compressor Theory and Operation

1. Bathie, W., Fundamentals of Gas Turbines,” Second Edition, John Wiley & Sons, Inc, 1996, pp. 348-367.
2. Fonda-Bonardi, G., “Turbocompressor for Vehicular Fuel Cell Service,” The 2000 Fluids Engineering Division Summer Meeting, paper #FEDSM00-11307, Boston, Massachusetts, June 11-15, 2000.
3. Ishino, M, et.al.,”Effects of Variable Inlet Guide Vanes on Small Centrifigal Compressor Performance,” Presented at the International Gas Turbine & Aeroengine Congress and Exhibition (ASME), Indianapolis, Indiana, June 7, 1999.
4. Milburn, S.M., “Introducing a High Efficiency Variable Positive Displacement Automotive Supercharger,” SAE Paper #940845, 1994.
5. Milburn, S.M., et.al., “A Variable Displacement Compressor/Expander for Vehicular Fuel Cell Air Management,” SAE Paper #961713, 1996.
6. Pischinger, S., et.al., “Integrated Air Supply and Humidification Concepts for Fuel Cell Systems,” Presented at the SAE 2001 World Congress, March 5-8, 2000, SAE # 2001-01-0233, 2001.
7. Roan, V.P., et.al., “Air System Technology Programs Review Panel,” Presentation at the U.S. Department of Energy Air Management Workshop, Argonne National Laboratory, October 10, 2000.
8. Sutton, R.D., “Compressor Technologies for PEM Fuel Cells,” Presentation at the U.S. Department of Energy Air Management Workshop, Argonne National Laboratory, October 10, 2000.
9. Wiartalla, A., et.al, “Compressor Expander Units for Fuel Cell Systems,” Presented at the SAE 2000 World Congress, March 6-9, 2000, SAE # 2000-01-0380, 2000.
10. “Development of a Turbocompressor for Fuel Cells in Transportation Applications,” Final report to U.S.Department of Energy by **AlliedSignal Inc**, 1998.
11. “Fuel Cell Turbocompressor,” Presentation to the U.S.Department of Energy by **AlliedSignal Inc.**, Washington D.C., June 25, 1998.
12. “Development of Compressor/Expander for Fuel Cells in Transportation Applications,” report to U.S.Department of Energy by **Arthur D. Little, Inc.**, Cambridge, Massachusetts, February 10, 1998.
13. “Scroll CEM Performance Overview,” **Arthur D. Little, Inc.**, Presentation at the U.S.Department of Energy Pressure Effects Workshop, Argonne National Laboratory, December 15, 1998.
14. “Balance of Plant Components,” Final report to U.S.Department of Energy by **Vairex Corporation**, Boulder, CO, April 6, 1998.
15. 1996 ASHRAE Systems and Equipment Handbook, pp. 34.24-34.25 (Trochoidal Compressors).

### **Compressor Modeling**

16. Kessel, J.A., et.al., "Modeling and Real-Time Simulation of a Turbocharger with Variable Turbine Geometry (VTG)," SAE Paper #980770, 1998.
17. Margolis, D, and S.Craig, "Bond Graph Modeling of a Scroll Compressor with Two-Phase Flow and Heat Transfer," University of California at Davis, report to Aisin Seiki Company Ltd.
18. Moraal, P., and Ilya Kolmanovsky, "Turbocharger Modeling for Automotive Control Applications," SAE Paper #1999-01-0908, 1999.
19. Nasser, S.H., and B.B.Playfoot, "A Turbocharger Selection Computer Model," SAE Paper #1999-01-0559, 1999.

### **Performance Mapping**

20. Kurzke, J., and Claus Riegler, "A New Compressor Map Scaling Procedure for Preliminary Conceptual Design of Gas Turbines", Presented at the International Gas Turbine & Aeroengine Congress & Exhibition (ASME), Munich, Germany, May 8, 2000.
21. Volponi, A.J., "Origin of the Gas Turbine Parameter Corrections for Ambient Conditions," Presented at the International Gas Turbine & Aeroengine Congress & Exhibition (ASME), Stockholm, Sweden, June 2-5, 1998.

### **Transients**

22. Brace, C.J., et.al., "Transient Investigation of Two Variable Geometry Turbochargers for Passenger Vehicle Diesel Engines," SAE Paper #1999-01-1241, 1999.
23. Brown, F.T., "The Transient Response of Fluid Lines," Journal of Basic Engineering, ASME, December 1962, pp. 547-553.
24. Kantola, R., "Transient Response of Fluid Lines Including Frequency Modulated Inputs," Journal of Basic Engineering, ASME, June 1971, pp. 274-281.
25. Schuder, C.B., and R.C.Binder, "The Response of Pneumatic Transmission Lines to Step Inputs," Journal of Basic Engineering, ASME, December 1959, pp. 578-584.

### **Fuel Cell Systems Analysis**

26. Barbir, F., "Air, Water and Heat Management in Automotive Fuel Cell Systems," Presented at the Commercializing Fuel Cell Vehicles 2000 conference, 12-14 April, 2000, Berlin, Germany.
27. Barbir, F., et.al., "Trade-off Design Analysis of Operating Pressure and Temperature in PEM Fuel Cell Systems," Proceedings of the ASME Advanced Energy Systems Division, AES-Vol. 39, ASME 1999.
28. Doss, E.D., et al., "Pressurized and Atmospheric Pressure Gasoline-Fueled Polymer Electrolyte Fuel Cell System Performance," Presented at the SAE 2000 World Congress, March 6-9, 2000, SAE # 2000-01-2574, SAE International, Warrendale, PA, 2000.
29. Eggert, A., et al., "Water and Thermal Management of an Indirect Methanol Fuel Cell system for Automotive Applications," Proceedings of the 2000 International Mechanical Engineering Congress and Exposition, Orlando, FL, November 5-10, 2000.

30. Friedman, D.J., R.M.Moore, "PEM Fuel Cell System Optimization", Proceedings of the Second International Symposium on Proton Conducting Membrane Fuel Cells II, Edited by S. Gottesfeld et al., Electrochemical Society, Pennington, NJ, 1999.
31. Friedman, D.J., A.Eggert, P.Badrinarayanan, J.M.Cunningham, "Maximizing the Power Output of an Indirect Methanol PEM Fuel Cell System: Balancing Stack Output, Air Supply, and Water and Thermal Management Demands," Presented at the SAE 2001 World Congress, March 5-8, 2001, SAE # 2001-01-0535, SAE International, Warrendale, PA, 2001
32. "Cost Analysis of Fuel Cell System for Transportation: Baseline System Cost Estimate," Task 1 and 2 Final Report to the Department of Energy by **Arthur D. Little Inc.**, March 2000, Ref. 49739

## ***4.2 Full copies of referenced papers from Part II***

### **4.2.1 Expander Implications: EVS-17 Conference 2000**

*This paper was presented with a poster presentation at the EVS-17 (Electric Vehicle Symposium) in Montreal, Quebec on October 17, 2000. The paper is published in the conference proceedings.*

---

## **THE IMPLICATIONS OF USING AN EXPANDER (TURBINE) IN AN AIR SYSTEM OF A PEM FUEL CELL ENGINE**

J.M. Cunningham  
M.A. Hoffman, A.R. Eggert, D.J. Friedman  
Institute of Transportation Studies  
Fuel Cell Vehicle Modeling Program  
University of California – Davis

### **Abstract**

This paper compares the performance of various air supply configurations in an automotive PEM fuel cell system. An air supply configuration that uses only a compressor will be compared to a system that incorporates an expander (turbine) for energy recovery in addition to the compressor. It is shown that the use of the expander (turbine) results in an improvement to the system efficiency at peak power levels. However, under normal driving conditions, peak power levels are demanded only a small fraction of the time. Therefore, it becomes less clear as to whether the added complexity of a turbine would be beneficial.

This paper examines the specific issues of fuel cell stack size and system efficiency at various net power levels for the two alternative options when a turbine is added. For option I, it is shown that by maintaining the same size stack while adding a turbine, *maximum* net power capability is improved by 14%. Net efficiency is improved by 4 to 5 percentage points near the maximum net power level but largely unchanged in the lower net power range. Conversely, for option II where the maximum net power is maintained the same, adding a turbine results in reducing the required stack size by 13%. However, net efficiency is reduced by 1 to 1.5 percentage points in the 15 to 35kW net power range. Unfortunately, this lower power region is where the vehicle operates most frequently under normal driving cycles. The details of these performance tradeoffs will be shown along with a discussion on cathode exhaust stream contents in general.

### **Keywords**

Compressor, Efficiencies, Electric Vehicle, Fuel Cell, PEM, Pressurized, System

### **Introduction**

The paper focuses on the use of a motor-assisted turbocompressor in the context of the fuel cell system, with and without exhaust gas energy recovery. The compression process provides pressurized air to the cathode reaction sites of the stack. Following the electrochemical reduction process at the cathode, the gas (a mixture of N<sub>2</sub>, unused O<sub>2</sub>, and water vapor), and any liquid water, exits the stack and the gas can be used in a turbine to recover shaft energy as the gases expand and cool. The difference in required compression energy is supplied by an electric motor.

For the purpose of the simulation in this paper, the interactions of the air system and the cathode gas stream in the fuel cell stack will be studied. Details of the water and thermal management auxiliaries will not be studied quantitatively in the simulation. However, a discussion will be presented regarding auxiliary size tradeoffs depending on the air system conditions.

Several system interactions will be addressed for the turbine configuration. First, the pressure loss across the stack channels will be accounted for, since this loss reduces the potential energy recovery in the turbine. Second, because the net parasitic power required in the compression process is reduced, the stack size necessary for a desired peak system power may be reduced. Third, the potentially significant impact of the water added to and generated in the cathode stream will be discussed.

This paper contains three primary sections. The Modeling Setup section is meant to be a tutorial of the important subsystems involved in the system study. The Simulation Description and Simulation Results sections provide examples of modeled system performance.

## **MODELING SETUP**

### **System Description**

This section will provide an overview of the subsystems and their interactions.

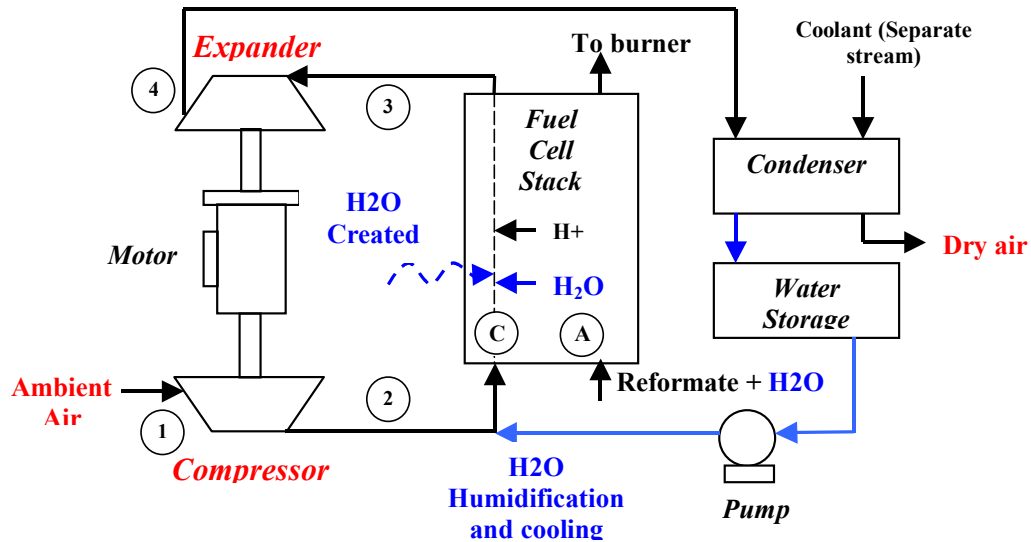


**Figure 1: Relevant System Diagram**  
*C = cathode, A = anode*

Figure 1 outlines the primary components necessary for this study. There are three primary subgroups of components in the system proposed: the fuel cell stack and the corresponding reactions at the cathode site; the air system which consists of the compressor, turbine, and electric motor; and the water and thermal management auxiliaries, namely the radiator, coolant pump, humidifier/vaporizer, condenser, and cooling fans (only condenser, humidification pump, and water storage are shown). The model used for this initial study investigates the interactions of the system described above but *does not* involve the vehicle simulation at this point.

### Air System

For this initial study, the air system used is a radial flow turbocompressor technology designed by Meruit Inc. The following performance map shows the relationship of the compressor output pressure ratio ( $r_c$ ) and air mass flow rate ( $\dot{m}_a$  in g/s).

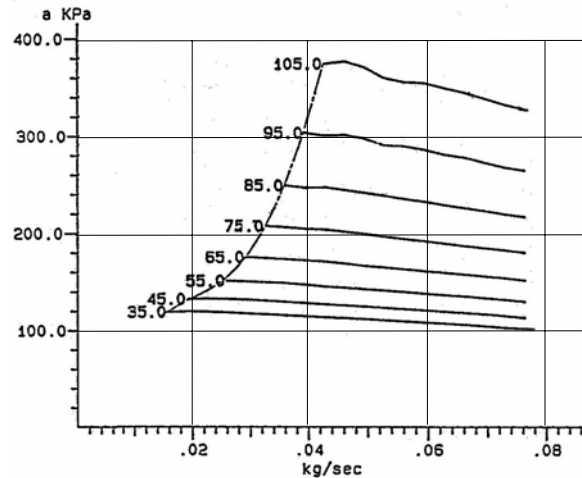


**Figure 2: Air compressor map,  $p$  (kPa) vs.  $\dot{m}_a$**

Power to the compressor shaft is supplied by a high-speed electric motor (AC induction) or by a combination of the motor and shaft power recovered by the radial inflow turbine. The following turbine map from Meruit Inc was generated for dry air with a fixed pressure loss in the fuel cell stack and piping between the compressor outlet and the turbine inlet assumed to be 0.22 atm.

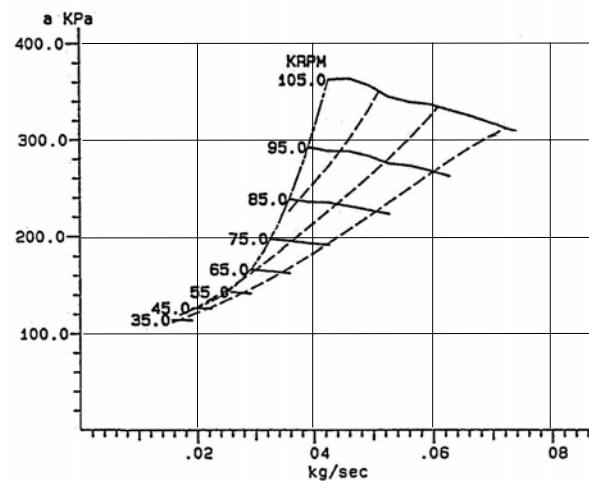


**Figure 3: Turbine map,  $p$  (kPa) vs.  $\dot{m}_a$**

Energy recovery from the turbine, when utilized, is dependent upon the gas mass flow exiting the fuel cell stack cathode and provided to the turbine.

In general, from the perspective of the air system performance, increased gas mass flow into the turbine in the form of water vapor (in the N<sub>2</sub> and O<sub>2</sub> gas flow) is beneficial for energy recovery. As the gases expand and cool down in the turbine work is transferred from the fluid stream to the turbine wheel. The gas mass flow is decreased but the heat of condensation is added to the gas (like internal reheat) as the water vapor condenses into the liquid state. This is in contrast to a system that extracts the water vapor content prior to the turbine. Details of how significant the water vapor content can be are discussed in the next section.

The following equations describe the *shaft* power performance of the compressor and turbine. The difference must be supplied by the electric motor.

$$P_{\text{sh-c}} = \dot{m}_a c_{pc} (T_2 - T_1) = \left( \frac{1}{\eta_{\text{isen-c}} \eta_{\text{mech-c}}} \right) \left( \dot{m}_a c_{pc} T_1 \left( r_c^{\frac{kc-1}{kc}} - 1 \right) \right) \quad (1)$$

$$P_{\text{sh-t}} = (\eta_{\text{isen-t}} \eta_{\text{mech-t}}) \left( \dot{m}_{\text{gas}} c_{pt} T_3 \left( 1 - r_t^{\frac{1-kt}{kt}} \right) \right) \quad (2)$$

In actual systems, it is not unusual for the outlet air temperature from a centrifugal compressor, T<sub>2</sub>, to exceed 150<sup>o</sup>C (for air at 3.0 atm, inlet at STP). This temperature range far exceeds the desired temperature of approximately 80<sup>o</sup>C of the fuel cell stack.

The water spray used to humidify the air flow is also used to cool it.

### **Cathode Stream Water Content**

The water vapor and liquid content in the flow is comprised of three components: 1) water formation as a result of the electrochemical reduction process at the cathode catalyst (“form”); 2) water injected into the cathode air flow for cooling purposes (a form of humidification – “hum”); and 3) water dragged with the H<sup>+</sup> ions across the membrane from the humidified anode stream (“drag”). The following equations describe the water content in the *cathode* flow.

$$\dot{n}_{o_2} = \frac{\dot{m}_a}{(4.76 * MW_a)} \quad (3)$$

$$\dot{n}_{h_2o-form} = \frac{2\dot{n}_{o_2}}{SR} \quad \text{and} \quad \dot{n}_{h_2-utilized} = \dot{n}_{h_2o-form} \quad (4)$$

(2 moles H<sub>2</sub>O formed for every 1 mole O<sub>2</sub> utilized in the air flow)

$$\dot{n}_{h_2o-drag} = 0.4 \dot{n}_{h_2-utilized} \quad (5)$$

(0.4 moles H<sub>2</sub>O dragged across membrane per 1 mole 2H<sup>+</sup> ions, constant value assumed for the PEM fuel cell modeled in this study)

$$\dot{n}_{h_2o-hum} = f(T_2, r_c, \dot{n}_a) \quad (6)$$

The resulting *total gas* mass flow into the turbine from the cathode exhaust, therefore, is the following:

$$\dot{m}_{total} = \left( \dot{n}_{o_2-unused} MW_{o_2} \right) + \left( \dot{n}_{n_2} MW_{n_2} \right) + \left( \left( \dot{n}_{h_2o-form} + \dot{n}_{h_2o-drag} + \dot{n}_{h_2o-hum} - \dot{n}_{h_2o-liq} \right) MW_{h_2o} \right) \quad (7)$$

The following table provides parameter values, for explanatory purposes, for one design point. The results include the cathode exhaust fluid flow contents for a cathode air operating stoichiometric ratio (SR) of 1.5.

**Table 1: Example cathode exhaust fluid stream contents**

	<i>PARAMETER</i>	<i>VALUE</i>
1	$r_c$	2.0 atm
2	• $m_a$ (dry air, compressor exit)	50.00 g/s
3	• $m_{h2o-form}$	8.70 g/s
4	• $m_{h2o-drag}$	3.48 g/s
5	• $m_{h2o-hum}$	1.24 g/s
6	% of water mass flow in vapor form	60 %
7	• $m_{o2-unused}$	3.87 g/s
8	• $m_{n2}$	38.17 g/s
9	• $m_{total}$ (gas into turbine, including water vapor <i>only</i> )	50.19 g/s
10	• $m_{total}$ (excluding H2O liquid <i>and</i> vapor)	42.04 g/s

- Notes:** 1) All  $m^*$  parameters were calculated by multiplying the “n\_” parameters by the respective constituent’s molecular weights (MW);  
 2) The water content exiting the cathode is a mixed flow, part vapor and part liquid.  
 3) H2O added for humidification based on temperature profile of Meruit compressor  
 4) The operating temperature of the stack is assumed to be maintained at 80°C

It is obvious that if the water vapor flow were to be condensed and extracted from the fuel cell cathode exhaust prior to the turbine, the gas mass flow into the turbine would be significantly reduced (by 16.2%) in the above example; line 10 vs. line 9). This is a large fraction of the total mass flow that would not be available for the turbine energy recovery.

The expander can play an integral role in water recovery for the system. As the gas expands and cools within the expander, water vapor may condense into liquid form and then be subsequently collected for use within the system. If the quantity of liquid water

that exits the expander is not sufficient for the system needs, a condenser must be used to condense the additional water required. Considering the expander reduces the pressure and temperature of the gas stream, it becomes more difficult to condense additional water because of the decreased saturation temperature and the decreased temperature difference between the gas stream and ambient air. In this case, even though the thermal load on the condenser ( $Q$ ) may be reduced, the auxiliary (condenser fan and/or pump) energy required may increase. Consequently, the expander could have the effect of either increasing or decreasing the energy requirement of the condenser. A detailed study is required to determine whether placing the condenser prior to or after the expander is the most efficient arrangement.

### **Pressure Loss**

The pressure drop between the inlet and exit of the cathode channels in the fuel cell stack ( $p_2 - p_3$ ) is assumed to be the dominant loss in pressure between the compressor exit and the turbine inlet. Significant effort by fuel cell stack developers is devoted to designing cathode flow fields that minimize this pressure loss. The loss in air pressure reduces the stack performance by way of reduced partial pressure of oxygen at the catalyst reaction sites near the exit of the cathode channels. The compressor performance is also impacted because it must make up the pressure loss. Additionally, total pressure of the fluid is reduced, impacting the potential benefits of the turbine. For this initial study a *fixed* pressure loss of 0.22 atm has been assumed between the compressor and the turbine.

## **Simulation Description**

### ***Modeling Description***

An optimization model, *independent* from a vehicle simulation model, has been created to determine the optimum operating scheme for the air system in the context of the fuel cell stack's cathode characteristics. Using the fuel cell stack's range of current density as the independent variable, the optimization code "searches" for the Pox (partial pressure of oxygen at the catalyst reaction sites) and air mass flow rate that will generate the maximum net electric power for each value of the current density. In doing so, cell voltage – current density characteristics are taken into account, and total air pressure is directly calculated from the optimum partial pressure of oxygen. The defined net electric power is simply the stack gross electric power minus the air system electric motor power required (calculated from the air system model during the optimization process). The *end result is a performance map* of the fuel cell stack / air system combination that provides net efficiency and net power for each value of current density. Additionally, the resulting pressure ratio and air mass flow, both of which vary with current density, are presented. Because the performance map is a result of the optimization process, this optimum operating scheme is unique to that particular air system and fuel cell stack.

The model uses air system performance data provided by air system developers such as Meruit Inc. The data are included in the model in the form of two-dimensional performance maps for shaft power, shaft speed, and exit air temperature. The fuel cell stack characteristics are directly modeled and have been validated against lab performance data from Los Alamos National Laboratory. The optimization performance

scheme is used, along with the compressed air temperatures, to determine the resulting water requirements of the system as previously described in this paper.

In an overall system study, these results from the optimization process are then incorporated into a separate full vehicle model to simulate transient performance over standard drive cycles. The results of *this initial study* are based on the optimization model *only*, and have not yet been incorporated into the vehicle simulation. The system's performance in the full vehicle model will be investigated in a future study.

### ***Components and Performance Maps***

For the purpose of this study, the “Base Case” is defined as the system configuration without a turbine. Specifically, the fuel cell stack for this case is scaled such that the maximum net power of the fuel cell stack and compressor is 50kW-electric. To achieve this, the fuel cell stack in the Base Case incorporates 350 cells with 420 cm<sup>2</sup> of active cell area each and has a maximum gross power of 62kW. The air system maps were provided by Meruit Inc. and are shown in Figures 2 and 3.

As mentioned previously, a turbine's energy recovery potential will increase if the water vapor content of the cathode exhaust is included. The previous section describing the water vapor and liquid content is provided as a tutorial and to show the potential use of the contents in the cathode exhaust. However, for the purpose of these initial simulations, only dry air will be considered. Note that this implies a change in the configuration shown in Figure 1. The condenser must now be placed *between* the fuel

cell stack and the turbine in order to have dry air flow in the turbine. The results of the simulation will provide useful information by showing some basic system tradeoffs.

The following three cases were modeled and will be referred to in the results and conclusion section:

**Table 2: Simulation Configurations**

<b>Configuration</b>	<b>Net Power</b>	<b># of cells</b>	<b>Active area per cell</b>	
• Base Case:	50 kW net;	350 cells;	420 cm <sup>2</sup> ;	no turbine
• Exp I:	> 50 kW net;	350 cells;	420 cm <sup>2</sup> ;	with turbine
• Exp II:	50 kW net;	<b>305</b> cells;	420 cm <sup>2</sup> ;	with turbine

The Exp I configuration is intended to show differences in system performance by adding a turbine *and* maintaining the same size stack. In contrast, the Exp II configuration takes advantage of the turbine to reduce the stack size while maintaining the same peak net power of 50kW as the Base Case.

For the purpose of this study, the following initial conditions were assumed:

- Ambient air relative humidity = 0
- Ambient air temperature and pressure were at STP: 25<sup>o</sup>C and 1 atm
- Input gas temp. to the turbine (thus cathode exit gas temp.) was 80<sup>o</sup>C

## **Simulation Results and Discussion**

### ***Primary Results***

Figure 4 shows the relationship of net efficiency to net power in all three simulations while Figure 5 shows the electric power as a function of current density. For the figures, the following relationships hold for the fuel cell stack gross electric power and air supply (as) electric motor power, respectively:

$$P_{stack\_gross} = (VI)_{stack} \quad ; \quad P_{as\_motor} = \frac{(P_{sh\_comp} - P_{sh\_exp})}{\eta_{as\_motor}} \quad (8)$$

$$P_{net} = P_{stack\_gross} - P_{as\_motor} \quad (9)$$

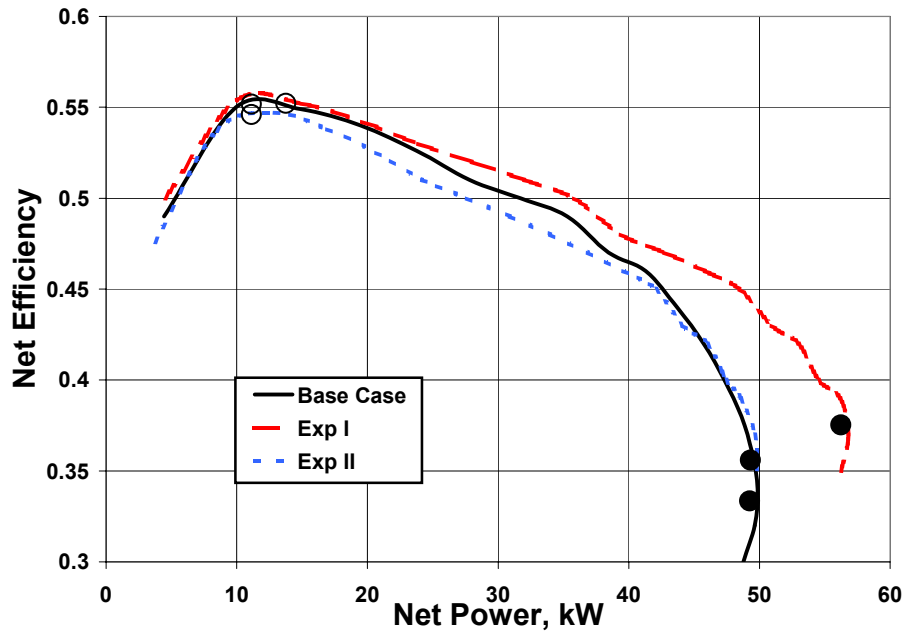


Figure 4: Net Efficiency vs. Net Power

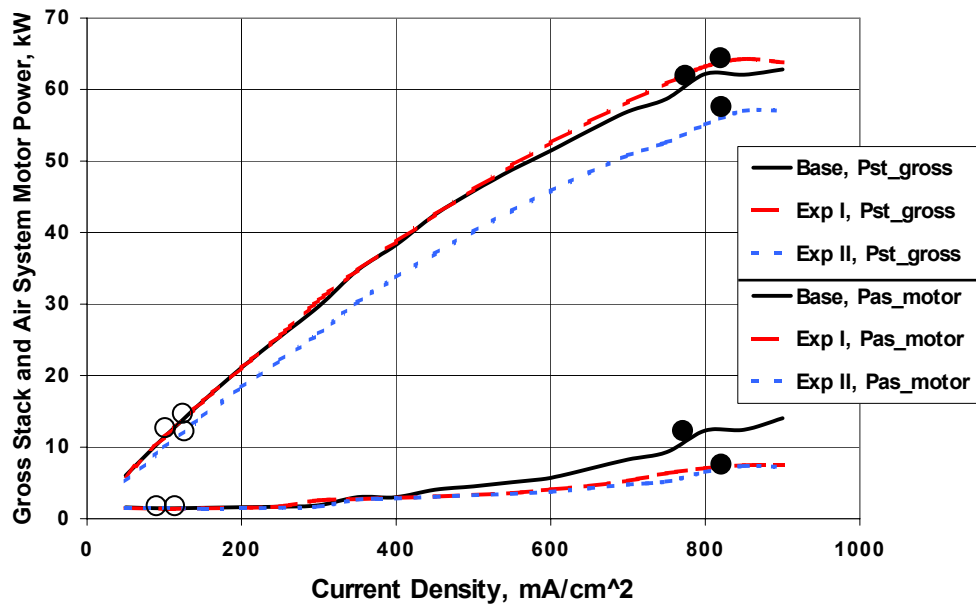


Figure 5: Electric Power vs. Current Density

Key: ● = 100% and ○ = 25% of peak net system power

In comparing the Base Case to the Exp I simulation, the first observation is that the *peak net* power capability has been increased by 14%. This is not surprising considering the stack size has not changed and thus the gross power is unaffected. Lower compressor electric motor (parasitic) loads, as shown in Figure 5, result in increased maximum net power capabilities.

The second observation with the Exp I configuration is that the net efficiency has noticeably improved for the high net power range of 25kW to 50kW yet almost unchanged for the low net power region where the vehicle is operated the majority of the time under standard driving cycles such as the FUDS and HIWAY. For the same net power output, the hydrogen used is less for the Exp I configuration in the higher power region resulting in increased net efficiency. This is also shown in Figure 5 where, for a given net power value, the current density is reduced for the expander configurations (primarily in the higher current density regions). The *tradeoff* for this configuration compared to the Base Case is one of packaging and complexity due to the addition of the turbine versus the benefits of higher efficiency and power near the peak power region.

The second turbine configuration, Exp II, reveals noticeably different results. The overall tradeoff to note is that stack size, and presumably stack cost, are reduced at the expense of net efficiency. Specifically, stack size is reduced by 13% in the number of cells used. Though not much different at the high net power region, net efficiency is reduced slightly compared to the Base Case in the low net power range by up to 1 to 1.5 percentage

points. Unfortunately, this is precisely the operating region most utilized in standard vehicle drive cycles.

The simplest way to understand the efficiency difference is to examine the general characteristics of a fuel cell stack and air supply's net efficiency relative to the net power capability. Efficiency rises and reaches a maximum in the lower net power region and then gradually decreases with increasing net power (this trend can be seen in Figure 4). In the Exp II configuration, the stack size is reduced along with its maximum gross power capability. This implies that for the same net power values as the Base Case, the stack in Exp II will be operating at higher gross power levels relative to its maximum capability. This pushes the stack into a slightly less efficient region.

The following figure shows the relationship between the air system power ratio and the gross stack electric power. The air system power ratio is defined as follows:

$$PowerRatio = \frac{P_{as\_motor}}{P_{stack\_gross}} \quad (10)$$

where  $P_{as\_motor}$  is the electric power into the air system drive motor

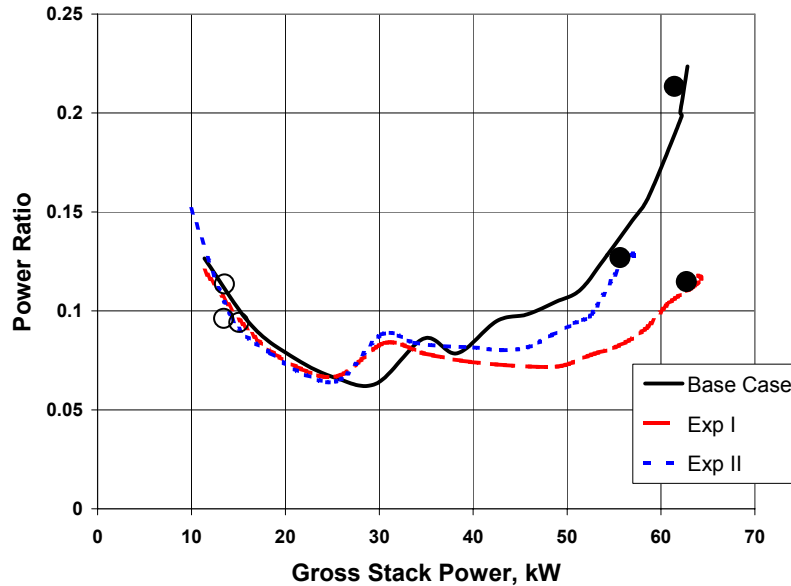


**Figure 6: Air system Power Ratio vs. Gross Stack Power**

At the high stack power region, the power ratio is reduced with the turbine configurations showing a reduced parasitic load for the air system. However, at low stack powers, the power ratios do not vary significantly between the configurations. At low pressure ratios and air flow rates, the turbine does not recover much energy.

Table 3 summarizes the performance parameters for two operating conditions: that of 100% power and of 25% part load power for each configuration.

**Table 3: Comparison of Configuration Performance\***

Parameter	Base Case	Exp I	Exp II
Stack gross power (kW)	62.18 (14.00)	64.28 (15.62)	57.06 (13.91)
Comp/turbine net electric power (kW)	12.32 (1.50)	7.47 (1.42)	7.25 (1.41)
System net power (kW)	49.86 (12.50)	56.81 (14.2)	49.81 (12.50)
Compressor pressure ratio	3.43 (1.26)	3.44 (1.27)	3.35 (1.26)
Compressor air mass flow rate (g/s)	65 (21)	76 (21)	76 (21)
Air stoichiometric ratio	1.55 (3.21)	1.70 (2.85)	1.84 (3.06)
Compressor efficiency **	0.74 (0.73)	0.72 (0.73)	0.71 (0.75)
Turbine efficiency **	-	0.88 (0.87)	0.88 (0.90)
Air system motor efficiency	0.90 (0.39)	0.90 (0.37)	0.89 (0.35)

\* Note: performance values are for the configuration's maximum *system net power* capability

[label ● on plots]. Values in ( ) are for 25% of system net power capability [label ○ on plots].

\*\* Efficiency values are defined at the common motor shaft and are equivalent to the isentropic efficiency multiplied by the mechanical efficiency of the device.

One parameter worth noting from Table 3 above is the air supply motor efficiency. For the part load condition, the efficiency values are very low. The motor characteristics used for this simulation were not optimized for the lower power regime. However, considering the vehicles operate in this power region the majority of the time, an improved motor is need for this model.

The air system efficiency values are were calculated as follows:

*Compressor efficiency at the shaft of the motor:*

$$\eta_{sh\_comp} = \eta_{isen} \eta_{mech} = \frac{m c_p T_1 (r_c^{(k_c-1)/k_c} - 1)}{m c_p (T_2 - T_1)} \eta_{mech} = \frac{m c_p T_1 (r_c^{(k_c-1)/k_c} - 1)}{P_{sh\_comp}} \quad (11)$$

*Turbine efficiency at the shaft of the motor:*

$$\eta_{sh\_exp} = \eta_{isen} \eta_{mech} = \frac{m c_p (T_3 - T_4)}{m c_p T_1 (1 - r_t^{(1-k_t)/k_t})} \eta_{mech} = \frac{P_{sh\_exp}}{m c_p T_1 (1 - r_t^{(1-k_t)/k_t})} \quad (12)$$

*Air supply motor efficiency (not including losses in power conditioning, i.e. controllers):*

$$\eta_{as\_motor} = \frac{(P_{sh\_comp} - P_{sh\_exp})}{P_{as\_motor}} \quad (13)$$

## Conclusions

The following results and trends have been shown:

- For the turbine configuration with the same size stack relative to the Base Case (Exp I):
  - The net efficiency is noticeably improved in the higher power region above 24kW net. Specifically, the net efficiency is improved by up to 4 percentage points at 45kWnet. However, net efficiency is almost unchanged in the lower power region.
  - Peak net power capability is increased by 14%
- For the turbine configuration with reduced stack size relative to the Base Case (Exp II):
  - The stack size is reduced by 13% while the peak net power capability is maintained
  - Noticeable reductions in net efficiency are apparent for much of the net power range. Specifically, between 15 and 35kW net power, the net efficiency for Exp II is reduced by 1 to 1.5 percentage points. Unfortunately, the lower power region is where the vehicle operates most of the time
  - Net costs would improve if the incremental cost reduction of the stack outweighs the increased cost of the turbine. Results from an ArthurDLittle cost study indicate that the incremental cost of the stack size far outweighs the cost of the air system components (1).

- A significant portion of the cathode exhaust flow is water vapor that can be useful in the turbine's energy recovery. For the design point example presented, 60% of the total cathode water mass flow was water vapor. This is equal to approximately 19% of the total cathode exhaust gas mass flow ( $N_2$ ,  $O_2$ , and  $H_2O_{vap}$  combined). Exactly how much the given water vapor could improve performance (calculated for dry air in this study) is a complex function of the condensation and heat release in the turbine. This will be the subject of future research.
- With the use of a turbine, air system control methods become more complex. The pressure and the air mass flow would be controlled by varying the compressor/turbine common shaft speed *and* by varying the geometry of the turbine (variable vane positions). These two parameters can be used to control the backpressure from the turbine (and thus fuel cell system operating pressure) as well as mass flow. In a system without a turbine, backpressure is controlled with a simple flow valve at the exit of the fuel cell stack (or possibly at the condenser exit). This valve may be necessary in a system with a turbine that does not incorporate variable geometry control.
- By adding a turbine, system complexity is increased. Specifically, the addition of an extra component alters volume (packaging) considerations. The reduction in stack and condenser size may offset the turbine volume but the packaging would still be different (in terms of shapes and component location).

In conclusion, it has been shown that the use of a turbine has its benefits and drawbacks. A developer's configuration of choice will depend on the magnitude of the tradeoffs between system costs, weight, volume and net performance.

## Acknowledgements

The work presented in this paper is supported by the Fuel Cell Vehicle Modeling Project at the Institute of Transportation Studies, University of California, Davis. Acknowledgements are given to team member P Badrinarayanan for his assistance in the water management work. The modeling process utilizes the Matlab Simulink™ programs. Turbocompressor performance data was provided by P. Fonda-Bonardi at Meruit Inc. of Santa Monica, CA.

## References

1. Arthur D. Little, Inc., "Cost Analysis of Fuel Cell System for Transportation: Baseline System Cost Estimate," Task 1 and 2 Final Report to the Department of Energy, March 2000, Ref. 49739
2. Barbir, F., et al., "Trade-off Design Analysis of Operating Pressure and Temperature in PEM Fuel Cell Systems," Proceedings of the ASME Advanced Energy Systems Division, AES-Vol. 39, ASME 1999
3. Cunningham, J.M., "Requirements for a Flexible and Realistic Air Supply Model for Incorporation into a Fuel Cell Vehicle (FCV) System Simulation," Presented at the SAE Future Transportation Technology Conference and Exposition, 17-19 August, 1999, SAE #1999-01-2912, SAE International, Warrendale, PA, 1999
4. Doss, E.D., et al., "Pressurized and Atmospheric Pressure Gasoline-Fueled Polymer Electrolyte Fuel Cell System Performance," Presented at the SAE 2000 World Congress, March 6-9, 2000, SAE # 2000-01-2574, SAE International, Warrendale, PA, 2000
5. Eggert, A., et al., "Water and Thermal Management of an Indirect Methanol Fuel Cell system for Automotive Applications," Proceedings of the 2000 International Mechanical Engineering Congress and Exposition, Orlando, FL, November 5-10, 2000 (pending)
6. Ferrall, J., et al., "Design and Development of an Air-Reformate PEM Fuel Cell Stack system for Light-Duty Vehicles," Presented at the SAE 2000 World Congress, March 6-9, 2000, SAE # 2000-01-1553, SAE International, Warrendale, PA, 2000

7. Friedman, D.J., et al., "PEM Fuel Cell System Optimization", Proceedings of the Second International Symposium on Proton Conducting Membrane Fuel Cells II, Edited by S. Gottesfeld et al., Electrochemical Society, Pennington, NJ, 1999
8. Wiarfalla, A., et al., "Compressor Expander Units for Fuel Cell System," Presented at the SAE 2000 World Congress, March 6-9, 2000, SAE # 2000-01-0380, SAE International, Warrendale, PA, 2000

### Nomenclature

$c_p$	= specific heat
$k_c$	= ratio of specific heats, compressor
$k_t$	= ratio of specific heats, turbine
$I$	= stack total current, amperes
$\dot{m}$	= mass flow rate
$\dot{n}$	= molar flow rate, moles/s
MW	= molecular weight, g/mole
$P_{sh}$	= shaft power, kW
$p$	= pressure, atm
$r_c$	= compressor pressure ratio = $p_{c2} / p_{c1}$
$r_t$	= turbine pressure ratio = $p_{t3} / p_{t4}$
SR	= stoichiometric ratio of air: ratio of <b>moles of <math>O_2</math> in the air per second</b> supplied to fuel cell stack vs. <b>moles of <math>O_2</math> per second</b> utilized at the corresponding stack power level (or fuel consumption rate)
$T_1$	= ambient and compressor inlet temperature, 25°C or 298K
$T_2$	= compressor exit temperature, Kelvins
$T_3$	= fuel cell stack exit and turbine inlet temperature, Kelvins
$V$	= stack total voltage, volts
$\eta_{isen}$	= isentropic efficiency
$\eta_{mech}$	= mechanical efficiency

### Subscripts:

c = compressor, t = turbine/expander, sh = shaft, drag =  $H_2O$  transported across the membrane, hum =  $H_2O$  for humidification of air into the fuel cell, form =  $H_2O$  formed at from the catalyst reactions

1 = inlet conditions to the compressor - atmosphere, 2 = exit conditions from the compressor and inlet to the fuel cell stack, 3 = exit conditions from the fuel cell stack and inlet to the turbine, 4 = exit conditions from the turbine - atmosphere

#### **4.2.2 High-Pressure vs. Low-Pressure: SAE World Congress 2001**

*This paper was presented with an oral presentation at the SAE World Congress in Detroit MI, March 6, 2001. The paper is published in SAE publications under the number shown below*

---

**2001-01-0538**

### **A COMPARISON OF HIGH-PRESSURE AND LOW-PRESSURE OPERATION OF PEM FUEL CELL SYSTEMS**

Joshua M. Cunningham, Myron A. Hoffman, David J. Friedman  
Institute of Transportation Studies  
Fuel Cell Vehicle Modeling Program  
University of California – Davis

Copyright © 2001 Society of Automotive Engineers, Inc.

#### **ABSTRACT**

This paper compares the merits of operating a direct-hydrogen fuel cell (DHFC) system using a high-pressure air supply (compressor) versus one using a low-pressure air supply (blower). Overall, for the system modeled, it is shown that there is no inherent performance advantage for either mode of operation at the DHFC stack level. However, in practical applications, as will be shown in this paper, a systems analysis (stack and air supply) of power and efficiency needs to be performed.

Equivalent PEM DHFC stack peak power values can be obtained using both high-pressure and low-pressure air supply systems. For each air supply configuration, air mass

flow and pressure operating conditions can be found that result in an equal value of the oxygen partial pressure at the cathode catalyst layer surface.

However, at the system level, the required air supply power needed to achieve the same DHFC stack performance values can be drastically different for high and low pressure operation. In order to compare the two systems, an optimal air supply control strategy is first developed to obtain the desired stack operating conditions with minimal parasitic loads based on each air supply configuration. Second, the resulting air supply parasitic loads are compared directly between the two configurations – both comparisons are set in the context of the system performance. In other words, the systems are sized such that the peak net power values are equal while the stack gross power may be different.

The results of the study demonstrate the well-known fact that equivalent DHFC peak net system power values (86kW) can be obtained with both types of air supply configurations but require different stack sizes. For the blower application, the stack size had to be increased by 16.3% (500 vs. 430 cells in this example) for a peak net power of 86kW. Differences are also apparent with the WTM sub-system. Quantitative results will be presented for both the high pressure and the low pressure applications.

## **INTRODUCTION**

Currently, fuel cell vehicles (FCVs) are being developed as a potential alternative to the conventional internal combustion engine vehicle (ICEVs). FCVs offer the potential of higher fuel efficiency and lower vehicle emissions compared to the ICEVs. However, an

area needing further development is a realistic systems analysis combining the various sub-systems and components for FCVs.

Depending on the output electrical power required from the fuel cell stack, the air mass flow rate and, in many stack designs, the pressure of the air will need to be varied. This acts to control the oxygen partial pressure at the cell reaction sites in order to produce a specific or desired "gross power" output from the fuel cell stack. Various air supply technologies are available, with varying performance capabilities, to provide the oxygen to the cathode sites. In general, the components can be separated into two categories: those of relatively high pressure ratio ( $r_c$ ) ability (compressors), and those of low pressure ratio ability (blowers). By operating the system at higher pressures, significantly more power is needed for the compressor operation. However, benefits can include higher stack efficiencies and smaller stack sizes/costs.

This paper seeks to compare the performance results and geometry of the system (fuel cell stack and air supply componentry) using both the compressor and the blower by scaling the fuel cell stack itself to obtain an equivalent peak net system power. The system modeled was that of a direct hydrogen fuel cell configuration.

## **MODELING SETUP**

The system performance results used for this paper's comparison were obtained by using the UC Davis computer simulation program created with Matlab's Simulink visual modeling software. The model uses air system performance data provided by air

component developers from actual lab tests. The data are included in the model in the form of two-dimensional performance maps for shaft power, shaft speed, and exit air temperature. The PEM fuel cell stack characteristics are directly modeled and have been validated against lab performance data from Los Alamos National Laboratory. Additionally, a water/thermal management (WTM) model was incorporated to account for condenser and radiator parasitic loads. The WTM model is based on fundamental relationships and data tables.

For the simulations, a twin-screw, positive displacement compressor from Vairex Corp. was chosen that has a maximum  $r_c$  capability of 2.5 and a maximum air mass flow of 105 g/s at an  $r_c$  of 1.8 (at STP conditions). For the low-pressure application, a “regenerative” blower from Siemens-Airtech was chosen which has a maximum  $r_c$  capability of 1.4 and a maximum air mass flow of 93 g/s at ambient pressure. The performance maps used in the model adequately account for the associated limitations of the particular technology (maximum and minimum performance regions). Additionally, a variable speed motor and controller map was utilized to determine the electric efficiency for the corresponding shaft speed and torque.

One unique feature of the model is the optimization procedure between the fuel cell stack performance, the parasitic load of the air supply technology utilized, and the parasitic loads of the condenser and radiator for the WTM system. The optimization in the model determines the air system operating scheme such that the net system electric power is

maximized for each value of the stack current density. A full description of this optimization procedure can be found in references [8, 9].

The defined net electric power is simply the stack gross electric power minus the parasitic loads of the air system electric motor (calculated from the air system model during the optimization process) and the WTM radiator and condenser loads. Equations 1 and 2 below specifically define these relationships.

$$P_{stack} = (VI)_{stack} \quad ; \quad P_{as\_motor} = \frac{(P_{sh\_comp})}{\eta_{as\_motor}} \quad (1)$$

$$P_{net} = P_{stack} - P_{as\_motor} - P_{rad} - P_{cond} \quad (2)$$

Note that the air system power in equation 1 is a function of the compressor load and does not include power recovered from an expander. Most pressurized systems will, however, incorporate an energy recovery device such as an expander. Performance data was not available to include the expander in this analysis. However, it has been shown that the use of an expander can reduce the air system power and stack size/cost [5].

The gross power of the fuel cell stack is directly dependent on the partial pressure of oxygen ( $p_{oxygen}$ ) at the cathode catalyst reaction sites. Each single value of  $p_{oxygen}$  corresponds to a single cell voltage value at each particular current density. However,  $p_{oxygen}$  is a function of both the total air pressure and the air mass flow rate, and can be achieved through different combinations of the two. Figure 1 shows this relationship for an *example* simulation (discussion purposes only). The figure shows a contour of constant  $p_{oxygen}$  values versus values for air pressure and air mass flow rate at a fixed

current density of  $400 \text{ mA/cm}^2$ . It can be seen that a wide range of pressures and air mass flows can achieve the exact same oxygen partial pressure, and therefore the exact same cell voltage (and therefore the exact same stack gross power). Thus, a high pressure system can achieve the same  $p_{\text{oxygen}}$  at low air flow rates that a low pressure system can achieve at high flow rates. It is therefore quite possible for both the compressor and the blower applications to produce the same partial pressure of oxygen and same stack gross output. For example, if the blower application has a limit in maximum output pressure, an increased amount of air mass flow compared to the compressor application can result in equal values of  $p_{\text{oxygen}}$ .

Equal stack gross powers do not, however, necessarily produce equal net system output powers. Instead, the proper  $r_c$  and air mass flow combination must be found to maximize the net system power at any given current density, compressor/blower choice, and specified  $p_{\text{oxygen}}$ . This will likely result in different air mass flow and  $r_c$  conditions for the blower and compressor applications. The resulting optimum choice takes into consideration the various component performance characteristics. (Note: the relationship between the current density and the mass flow is dependent on the air stoichiometric ratio)

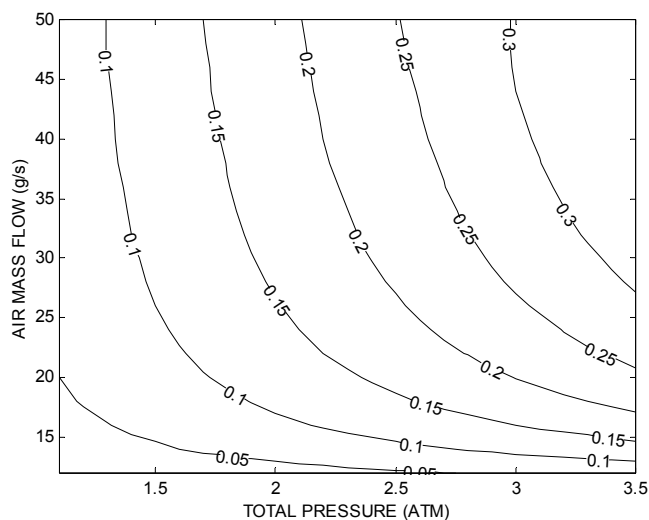


**Figure 1: Lines of constant Partial Pressure of Oxygen for a range of air mass flow (g/s) vs. total pressure (atm)**

**Note: fixed current density,  $J=400\text{mA/cm}^2$**

In addition to the stack / air supply interactions, the water and thermal management systems need to be considered. As described in reference [5], water is introduced to the cathode from several sources. It is dragged across the membrane from the anode (drag) along with the hydrogen ions, it is formed at the cathode reaction sites (form), and in some configurations it is directly injected into the air stream for cooling purposes, humidifying the stream in the process (hum). Two factors are important to study here. First, different  $r_c$  / air mass flow combinations require different total amounts of water for the same net power level. This can occur if the corresponding stack current is different for the various control schemes, and/or if the humidification needs are different depending on the exhaust air temperature from the compressor or blower. Second, different  $r_c$  / air mass flow combinations lead to different water states (%vapor vs. %liquid) in the fuel cell exhaust. Both of these factors have ramifications on condenser and radiator loads and will affect pump and fan (parasitic) electric loads. Again, refer to

the following references for modeling the WTM sub-systems and the related performance optimization procedure [1, 7, 9].

### **SIMULATION DESCRIPTION - HIGH Pressure vs. LOW Pressure**

The following table outlines the air system used along with the corresponding fuel cell stack characteristics modeled. Notice that in order to achieve the same net power, the blower application corresponds to a larger stack size, modeled as an increase in the number of cells while maintaining the same cell active area.

**Table 1: Simulation Input Parameters**

<b>Configuration</b>	<b>Net Power</b>	<b>#Cells</b>	<b>AA/cell</b>
Twinscrew Comp.	86 kW	430	490 cm <sup>2</sup>
Regenerative Blow.	86 kW	500	490 cm <sup>2</sup>

The specific stack size chosen was partially dependent on the voltage restrictions of the vehicle drive motor. In the UCDavis vehicle model, the drive motor operated properly if the voltage supply is held between approximately 200 – 400 volts during normal operation. With this restriction, a cell active area was chosen such that the number of cells for both the compressor and the blower applications resulted in adequate stack voltages.

It should be noted that to truly optimize a low pressure or high pressure system, the fuel cell stack for each application could be significantly different in physical design (i.e. cathode flow fields carefully designed to minimize total pressure losses for the blower application). This simulation was limited to simply varying the number of cells and therefore, conclusions from the study are somewhat limited as a result.

Figure 2 shows the system configuration including the primary components involved and the distribution of water in the system. More specific details regarding the WTM components can be found in reference [9].

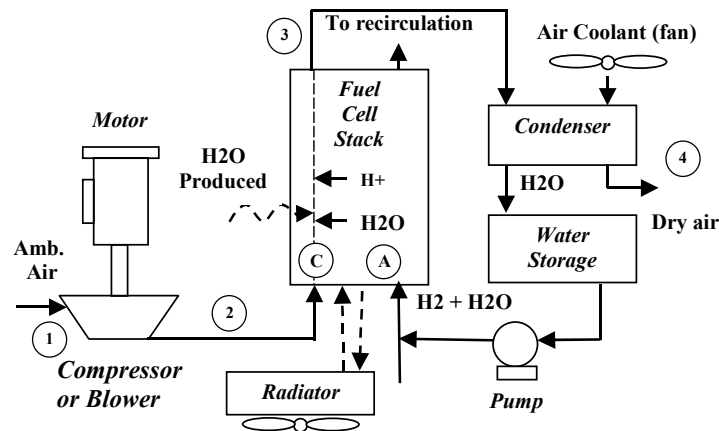
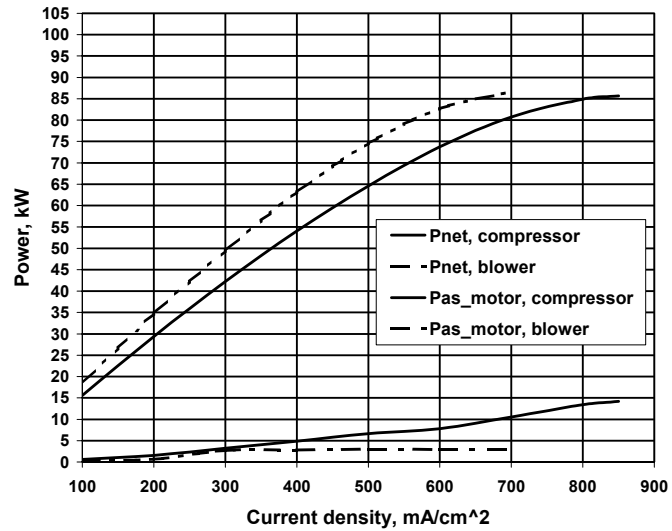


Figure 2: DHFC System Diagram

## SIMULATION RESULTS

### *Air System and Fuel Cell Stack Interactions:*

In Figure 3, the net system and air supply electric powers are graphed for the range of stack current density ( $\text{mA}/\text{cm}^2$ ). Both the blower and the compressor modeled provided the same peak  $P_{\text{net}}$  of 86 kW ( $P_{\text{stack}} - P_{\text{as\_motor}} - (P_{\text{cond}} + P_{\text{rad}})$ ). For the blower application, this range of net power occurred with lower parasitic loads (blower electric power) due to its lower pressure ratio operation (as shown in later figures). As a result, the peak net system power occurred at a lower gross stack power compared to the high pressure application. The major difference was that the blower required a stack with 16.3% more cells resulting in a costlier stack. Also note that the  $P_{\text{net}}$  values occurred at different stack current densities.



**Figure 3: Fuel Cell Stack Gross and Air System Electric Power**

Figure 4 shows the various power characteristics for the peak load condition (WTM parasitic loads not shown). It is evident that the blower's parasitic load is significantly less than that of the compressor at peak power.

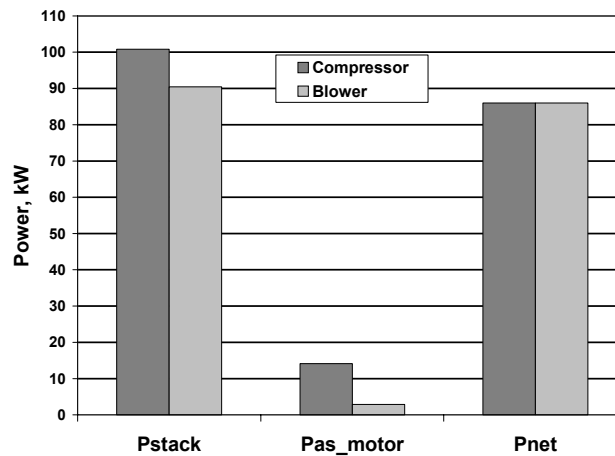


**Figure 4: Fuel Cell Stack peak gross and net power, and air system electric power**

Table 2 describes the efficiency relationships of the system.

**Table 2: System Power and Efficiency**

Parameter	Compressor	Blower
P <sub>net</sub> , kW	85.7 (18.0)	86.6 (18.4)
P <sub>as_motor</sub> , kW	14.2 (0.8)	2.9 (0.4)
Ratio P <sub>as_motor</sub> /P <sub>stack</sub>	0.14 (0.04)	0.03 (0.02)
Efficiency_stack(LHV) %	45.7 (62.3)	42.9 (62.4)
Efficiency_net, %	38.9 (59.6)	41.1 (61.0)

\* Values in ( ) are for part load performance, approximately 21% of peak net power

The efficiencies are defined as follows:

$$\eta_{stack} = \frac{P_{stack}}{\dot{m}_{H_2} * LHV_{H_2}} \quad (5)$$

$$\eta_{net} = \frac{P_{net}}{\dot{m}_{H_2} * LHV_{H_2}} = \eta_{stack} * \left(1 - \frac{(P_{as\_motor} + P_{rad} + P_{cond})}{P_{stack}}\right) \quad (6)$$

For both technologies, the net efficiency for the P<sub>net</sub> range was similar while achieving the same peak P<sub>net</sub>. The blower application maintained a  $\eta_{net}$  1.5-2.0 percentage points higher than the compressor application over the entire P<sub>net</sub> range. Both applications resulted in similar net efficiency variations of a typical fuel cell application where the peak efficiency occurs at the lower end of the P<sub>net</sub> range and slowly tapers off as power is increased.

The small difference in  $\eta_{net}$  can be understood by looking at Equation 6 and Figure 3.

For the same P<sub>net</sub>, if  $\dot{m}_{H_2}$  is lower,  $\eta_{net}$  increases. This was the case for the blower application. Figure 3 shows that current density (directly proportional to  $\dot{m}_{H_2}$  for a fixed utilization of hydrogen at the anode) was lower for nearly all stack power levels, and it can be shown that this relationship holds for the net system power as well.

But why was the current density lower? For a lower pressure in the fuel cell, the concentration of oxygen at the cathode catalyst is reduced. The low pressure application (given a fixed cell active area) makes up for this by increasing the number of cells per stack and thus total stack voltage.

Considering the similarity in  $\eta_{\text{net}}$ , both of these technologies would perform in a similar manner over a vehicular driving cycle where vehicle fuel economy over the range of engine power is a key performance parameter. However, other important differences may lead to dissimilar vehicle fuel economy. For instance, stack voltage differences at the same system net power and efficiency may result in different vehicle motor efficiencies and overall performance. Additionally, the transient response of the compressor or blower to vehicle load demands may differ impacting vehicle performance. Physical mass differences of the two systems will also impact vehicle response for a given system net power capability.

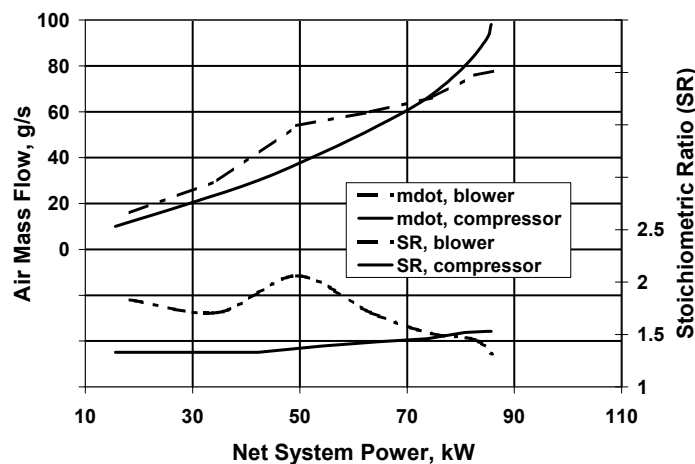


**Figure 5: Air mass flow rate and SR for the compressor and Blower**

Figure 5 shows the air mass flow rate as a function of the net power. For both applications, the air mass flow increases with power. However, for the blower, the air

mass flow requirements are higher over most of the power range to provide the optimum partial pressure of oxygen at the cathode catalyst sites with a corresponding lower total air pressure.

Also shown in the figure is the cathode air stoichiometric ratio (SR). This is a quantitative measure of the excess air mass flow in the stack required from the air supply. Considering the blower is limited in output pressure and compensates for this with sufficiently higher mass flows, the SR is higher for much of the net power range. The compressor, on the other hand, shows a relatively constant SR of 1.5.

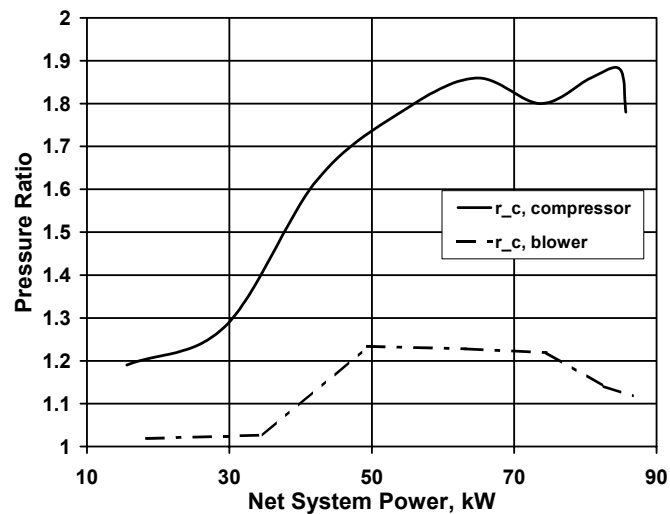


**Figure 6: Exit pressure of the compressor and blower**

Figure 6 shows the resulting pressure ratio operation for the air supply systems. The Blower operated near ambient pressure part of the time with a slight increase in pressure between 35 and 75kW(net). The compressor, on the other hand, shows a steadily increasing  $r_c$ , operating between 1.2 and 1.9 pressure ratios.

Also modeled in the simulations were pressure drops. At the high power levels, the air mass flow was larger leading to an increased pressure loss across the fuel cell. The pressure loss was much more restrictive to the blower application which already operated *near* ambient pressure. In these simulations, if the pressure loss characteristic had been larger, the blower system would not have obtained a net power of 86kW. This is an important consideration when performance matching a fuel cell stack and an air supply and why geometry would likely change.

In general, the non-linear performance curves in Figures 5 and 6 of both the air mass flow and  $r_c$  are a direct result of the optimization model which searches for the air supply air mass flow and  $r_c$  combination that maximizes the net power for a given current density. The resulting non-linear curve is unique to the specific compressor or blower and is dependent on the component's operating efficiencies.

It is important to note that all of the high pressure application results would differ if an expander were to be included.  $P_{net}$  would be achieved at reduced  $P_{stack}$  powers and thus different air pressure and mass flow schemes. Stack size would be further reduced, potentially increasing overall power density. Net system efficiency *may* improve as well.

#### ***Water and Thermal Management Interactions:***

As mentioned in the modeling section above, management of the water and thermal loads is critical in fuel cell systems. Ensuring that the fuel cell stack is adequately humidified is necessary, requiring the recovery of liquid water from the fuel cell stack exhaust by using water traps and condensers. Table 3 below shows the amount of water involved at

the maximum load condition for both the compressor and blower application. The data presents the conditions at the stack cathode exit.

**Table 3: Conditions at stack exit – Comparison at peak load condition**

Parameter	Compressor	Blower
P <sub>net</sub> , kW	85.7	86.6
P <sub>stack</sub> , kW	100.8	90.4
Current density, mA/cm <sup>2</sup>	850	700
Total current, A	417	343
r <sub>c</sub> , at the exit of the stack	1.8	1.01
Air stoichiometric ratio	1.5	1.3
$\dot{m}_{h_2o-form}$ , g/s	19.4	16.0
$\dot{m}_{h_2o-drag}$ , g/s	4.0	3.2
$\dot{m}_{h_2o-hum}$ , g/s	1.1	0.8
$\dot{m}_{h_2o-total}$ , g/s vapor and liquid	24.5	20.0
% of exit water mass flow in vapor form	88 %	100 %

\* Note: Assumes dry air into compressor inlet and a stack operating temperature of 80°C

Several trends can be seen in the results. The total water involved was lower for the low pressure, blower system. This is largely because  $\dot{m}_{h_2o-form}$  and  $\dot{m}_{h_2o-drag}$  are reduced due to lower current densities at the same net power. Additionally, the actual air mass flow utilized in the stack at the peak condition of 86kW(net) was less for the blower application in these simulations (total air mass flow divided by SR). However, since the pressure was lower at the exit of the fuel cell stack where the gas temperature was approximately 80°C, the percentage of water in the vapor form was higher for the blower application (100% vs. 88% for the compressor). Note that 100% of the water was in vapor form for the blower application at peak load because the gas temperature of 80°C was higher than the saturation temperature.

In these simulations, the actual amount of water that was needed for system operation (operating self-sufficiency) was simply  $\dot{m}_{h_2o-drag}$  (4.01g/s for the compressor and 3.24g/s for the blower applications). Consequently, even though the amount of system water required for the blower application was lower in these simulations, all of the water must be condensed at the condenser (as compared to the stack) and at a lower pressure. This has the effect of increasing the condenser load, resulting in either a larger condenser area and/or an increased cooling load on the condenser fan compared to the high pressure application. Additional details of the effects of cathode pressure on the condenser and radiator loads, and the associated tradeoffs, are discussed in reference [9].

Though not modeled, one possible way to increase the percentage of liquid water exiting the stack at the low pressure is to operate the fuel cell stack at lower temperatures. This has the effect of shifting the condensation load from the condenser to the radiator but also reducing stack efficiency.

***Physical Size/Geometry Considerations:***

As mentioned previously, the load on the condenser is dependent on several parameters, including the total quantity of vapor to condense and the gas stream pressure and temperature conditions. Comparing the low vs. high pressure systems at peak system load, the blower application operates with more water vapor exiting the stack at a lower gas pressure, both of which increase the condenser loads. To compensate for this, the condenser size and/or the fan load must be increased to extract the required amount of liquid water.

As shown, the fuel cell stack size was different as well. With the blower application, the total number of cells necessary in the stack was 16.3% larger than that needed for the pressurized system (500 vs. 430 cells), resulting in a larger stack size and cost. These stack size differentials are based on the same active area of  $490\text{cm}^2$  per cell for both applications.

The actual size of the compressor and the blower are assumed to be similar. If an expander were to be added to the pressurized application, the compressor/expander module may be larger. However, with the use of an expander, the stack size could be further reduced while still maintaining the same net power [5], and the condenser load may also be reduced if a significant portion of the vapor in the gas stream condenses in the expander (assuming the condenser is placed after the expander).

It was not possible, based on the current data, to determine which system has the larger volumetric power density ( $86\text{kW} / (\text{total system volume, m}^3)$ ). However, it is anticipated that the low pressure system will be larger in physical size due to the stack size differential and potentially larger WTM components. This would result in a lower volumetric power density.

## **CONCLUSIONS**

The following conclusions can be made from these specific simulations:

6. The same peak  $P_{\text{net}}$  can be achieved with both a blower (low pressure) and a compressor (high pressure), but the required fuel cell stack sizes are different. For the

- same peak  $P_{\text{net}}$  of 86kW, 16.3% more operating PEM cells were needed in the stack for the blower application (500 vs. 430 cells with a constant active area of 490cm<sup>2</sup>).
7. The blower system was able to obtain the same net power by operating just above ambient pressure at the stack and providing sufficiently higher air mass flow rates compared to that of the compressor for much of the  $P_{\text{net}}$  range.
  8. The parasitic loads for the blower are significantly less than that of the compressor at the high  $P_{\text{net}}$  region. The ratio of  $P_{\text{as\_motor}}/P_{\text{stack}}$  was 14.1% for the compressor vs. 3.2% for the blower at a peak  $P_{\text{net}}$  of 86kW (though these occur at different  $P_{\text{stack}}$  values).
  9. Overall, the net system efficiencies over the  $P_{\text{net}}$  range were very similar for both the blower and the compressor. However, the blower system did maintain a net efficiency 1.5 – 2.0 percentage points higher than the compressor system over most of the net power range.
  10. High pressure application results would differ if an expander were to be included.  $P_{\text{net}}$  would be achieved at reduced  $P_{\text{stack}}$  powers and thus different air pressure and mass flow schemes. Stack size would be further reduced, potentially increasing overall power density. Net system efficiency *may* improve as well.

## ACKNOWLEDGEMENTS

The work presented in this paper was supported by the Fuel Cell Vehicle Modeling Project at the Institute of Transportation Studies, University of California, Davis. The modeling process utilizes the Matlab/Simulink programs. The authors would also like to acknowledge the support received from Vairex Corp. and Siemens-Airtech in the

development of the air supply performance. Acknowledgements are given to team members P Badrinarayanan and Anthony Eggert for their assistance in the water and thermal management work.

## REFERENCES

1. Badrinarayanan, P., A.Eggert, K.H. Hauer, "Implications of Water and Thermal Management Parameters in the Optimization of an Indirect Methanol Fuel Cell System," Presented at the 35<sup>th</sup> Intersociety Energy Conversion Engineering Conference, 24-28, July 2000, Paper # 2000-3046.
2. Barbir, F., "Air, Water and Heat Management in Automotive Fuel Cell Systems," Presented at the Commercializing Fuel Cell Vehicles 2000 conference, 12-14 April, 2000, Berlin, Germany.
3. Barbir, F., et al., "Trade-off Design Analysis of Operating Pressure and Temperature in PEM Fuel Cell Systems," Proceedings of the ASME Advanced Energy Systems Division, AES-Vol. 39, ASME 1999
4. Cunningham, J.M., D.J.Friedman, M.A.Hoffman, R.M.Moore, "Requirements for a Flexible and Realistic Air Supply Model for Incorporation into a Fuel Cell Vehicle (FCV) System Simulation," Presented at the SAE Future Transportation Technology Conference and Exposition, 17-19 August, 1999, SAE #1999-01-2912, SAE International, Warrendale, PA, 1999
5. Cunningham, J.M., M.A.Hoffman, "The Implications of Using an Expander (Turbine) in an Air System of a PEM Fuel Cell Engine," Presented at the 17<sup>th</sup> International Electric Vehicle Symposium & Exposition, 15-18 October, 2000, Montreal Quebec.
6. Doss, E.D., et al., "Pressurized and Atmospheric Pressure Gasoline-Fueled Polymer Electrolyte Fuel Cell System Performance," Presented at the SAE 2000 World Congress, March 6-9, 2000, SAE # 2000-01-2574, SAE International, Warrendale, PA, 2000
7. Eggert, A., et al., "Water and Thermal Management of an Indirect Methanol Fuel Cell system for Automotive Applications," Proceedings of the 2000 International Mechanical Engineering Congress and Exposition, Orlando, FL, November 5-10, 2000 (pending)
8. Friedman, D.J., R.M.Moore, "PEM Fuel Cell System Optimization", Proceedings of the Second International Symposium on Proton Conducting Membrane Fuel Cells II, Edited by S. Gottesfeld et al., Electrochemical Society, Pennington, NJ, 1999
9. Friedman, D.J., A.Eggert, P.Badrinarayanan, J.M.Cunningham, "Maximizing the Power Output of an Indirect Methanol PEM Fuel Cell System: Balancing Stack Output, Air Supply, and Water and Thermal Management Demands," Presented at the SAE 2001 World Congress, March 5-8, 2001, SAE # 2001-01-0535, SAE International, Warrendale, PA, 2001

## NOMENCLATURE

I	= stack total current, A
J	= stack current density, A/cm <sup>2</sup>
$\dot{m}$ or $\dot{m}$	= mass flow rate, g/s
P	= power, kW
p	= pressure, atm
p <sub>oxygen</sub>	= partial pressure of oxygen
r <sub>c</sub>	= compressor pressure ratio = p <sub>c2</sub> / p <sub>c1</sub>

- SR = stoichiometric ratio of air: ratio of *moles of O<sub>2</sub> in the air per second* supplied to fuel cell stack vs. *moles of O<sub>2</sub> per second* utilized at the corresponding stack power level (or fuel consumption rate)
- T<sub>1</sub> = ambient and compressor inlet temperature, 25°C (298K)
- T<sub>2</sub> = compressor exit temperature, Kelvins
- T<sub>3</sub> = fuel cell stack exit and turbine inlet temperature, Kelvins
- V = stack total voltage, volts
- η = efficiency

Subscripts:

- as\_motor = air supply motor characteristic
- c = compressor
- cond = condenser
- drag = H<sub>2</sub>O transported across the membrane
- form = H<sub>2</sub>O formed at from the catalyst reactions
- hum = H<sub>2</sub>O for humidification of air into the fuel cell
- rad = radiator
- sh = shaft
- t = turbine/expander
- 1 = inlet conditions to the compressor –atmosphere
- 2 = exit conditions from the compressor and inlet to the fuel cell stack
- 3 = exit conditions from the fuel cell stack and inlet to the turbine
- 4 = exit conditions from the turbine - atmosphere

### **4.2.3 Air Supply Model Characteristics: SAE FTT Conference 1999**

*This paper was presented with an oral presentation at the SAE Future Transportation Technology Conference in Costa Mesa, CA, August 18, 1999. The paper is published in SAE publications under the number shown below*

---

**1999-01-2912**

## **REQUIREMENTS FOR A FLEXIBLE AND REALISTIC AIR SUPPLY MODEL FOR INCORPORATION INTO A FUEL CELL VEHICLE (FCV) SYSTEM SIMULATION**

Joshua M. Cunningham, Myron A. Hoffman, David J. Friedman  
Institute of Transportation Studies  
Fuel Cell Vehicle Modeling Program  
University of California – Davis

Copyright © 1999 Society of Automotive Engineers, Inc.

### **ABSTRACT**

This paper addresses the critical need to incorporate realistic models of the air supply sub-system in fuel cell system performance analysis. The paper first presents the dominant performance issues involved with the air supply operation in the fuel cell system. The report then goes on to propose a methodology for an air supply model that addresses many of the performance issues. Most importantly, a model is needed with a defined set of performance criteria and data input format, one that can accommodate multiple air supply configurations, and one that realistically and accurately simulates the air supply operation and its effect on the system power and efficiency. The paper

concludes that it is possible to compare alternative air supply components under the constraint of maximizing the instantaneous net fuel cell system efficiency for a dynamic vehicle driving cycle under various ambient conditions.

## **INTRODUCTION**

Currently, fuel cell vehicles (FCVs) are being developed as a potential alternative to the conventional internal combustion engine vehicles (ICEVs). FCVs offer the potential of higher fuel efficiency and lower vehicle emissions compared to the ICEVs. However, an area needing further development is a realistic systems analysis combining the various sub-systems and components. Though large performance improvements have occurred in the development of the fuel cell stack, a sub-system such as the air supply, which provides a mass flow of pressurized air to the fuel cell stack, needs careful scrutiny and development in conjunction with the fuel cell stack. A fuel cell stack alone may have good performance characteristics, but if the required air mass flow rate and air pressure are not attainable, the good performance will not be realized in a vehicle application.

This paper begins with a brief overview of the air supply requirements imposed by the fuel cell stack characteristics and outlines the air supply in the context of the total fuel cell system. The next section proposes a list and discussion of some dominant system performance issues that need resolution in order to maximize the interaction between the air supply and the fuel cell stack. The paper then proposes a methodology for an air supply model that will address the most important issues listed in the previous section. Examples are provided in the methodology for a specific type of compressor technology

and results include air supply performance as well as fuel cell system performance. Finally, future improvements to the model are mentioned.

## **FUEL CELL SYSTEM OVERVIEW**

The heart of a fuel cell vehicle is the fuel cell stack component. The fuel cell stack is an electrochemical device that generates electricity directly through the use of two catalytic processes involving the electrochemical oxidation of a fuel, for example hydrogen, and the electrochemical reduction of the oxygen in air. Depending on the output electrical power required from the fuel cell stack, the mass flow rate and, in many stack designs, the pressure of the air will need to be varied to control the oxygen partial pressure in order to produce a specific or desired "gross power" output from the fuel cell stack.

The pressurized air flow is a result of a compression process that requires input energy. The electrical power required to compress the air must be subtracted from the "gross power" of the fuel cell stack. The fuel cell stack gross power minus the power of the air supply is thus titled the "net system power" (currently, this net power does not include recovered energy through the use of an expander unit). This implies the need to compare various air supply technologies. By maintaining the same fuel cell stack characteristics, the system performance results from the use of varying air supply technologies can be studied. The two dominant performance characteristics are the net system power and the net system efficiency.

$$P_{\text{net\_system}} = P_{\text{gross\_stack}} - P_{\text{comp}} \quad [1]$$

$$\eta_{\text{net\_system}} = P_{\text{net\_system}} / [(\text{LHV of H}_2) \cdot \dot{m}_{\text{H}_2}] \quad [2]$$

where  $P$  represents "power" and  $LHV$  is the lower heating value per unit mass of fuel

Figure 1 below shows the relationship between the net system efficiency and the net system power for a particular fuel cell stack and air supply technology. The plot includes curves that represent constant pressure and air stoichiometric ratios. Though the process of optimizing the control scheme of the system to maintain the maximum efficiency for every given power is not the focus of this paper [Reference 1], this type of plot is a good comparison tool for the performance of various air supply technologies. Each air supply technology should be optimized in the system model (optimum choice of pressure and air mass flow or stoichiometric ratio) to provide the maximum net efficiency over the entire net power spectrum. The various system results can then be compared. It is important to point out, however, that the optimization described above may not need to occur when short bursts of high power are demanded of the system.

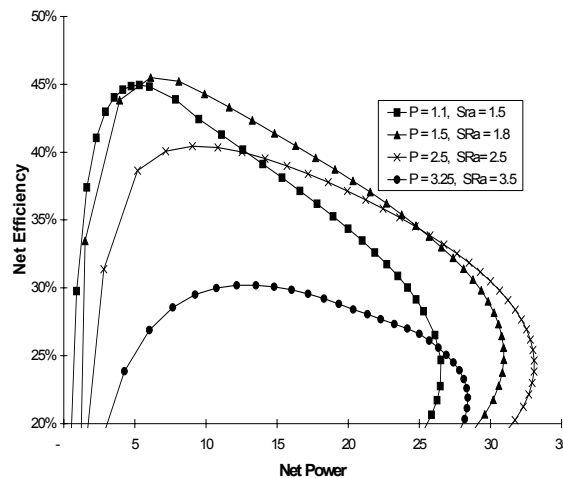


**Figure 1: Net system efficiency vs. Net system power**  
 Note: In this chart,  $P$  = pressure and  $Sra$  = stoichiometric ratio

## DOMINANT SYSTEM PERFORMANCE ISSUES

Considering the complexity of the performance interaction between the fuel cell stack and the air supply and considering its new application to the transportation sector, there are a number of open issues to address. This section provides a list and discussion of the dominant issues involved. It is important to note that the authors do not propose to fully answer all of the questions/issues. Rather, as stated previously, the goal of this paper is to raise the issues and then to propose one type of a solution. The section following will propose one type of methodology and model that addresses the performance issues.

- ***Is there an optimum fuel cell stack inlet air pressure ratio (PR) and mass flow rate (mdot) combination for maximum stack efficiency over the power spectrum?*** There is no single "optimum PR-mdot" combination for all fuel cell stacks. The combination will depend on the individual fuel cell stack in question. Furthermore, the "optimum PR-mdot" combination used should be that which maximizes the net fuel cell system efficiency for each net system power value (as opposed to the gross stack power and efficiency). This implies that the PR-mdot combination is also dependent on the parasitic losses attributed to the air supply system.
- ***What is the anticipated pressure drop in the fuel cell stack?*** The pressure drop will depend on both the fuel cell stack size (length and size of cathode side channels) and on the air mass flow rate. With optimized stack flow channels, the pressure drop may be small, yet should always be considered.
- ***Should an expander be incorporated?*** The use of an expander has several benefits and detriments. Primarily, it can be used to recapture energy from the pressurized, high mass flow, fuel cell stack exhaust gas. However, it adds complexity to the

system control scheme (i.e. accurately controlling system air pressure for the stack) as well as physical volume and mass. Therefore, the choice to use an expander will depend on whether there is enough energy in the exhaust flow and on vehicle packaging. In the modeling procedure, expander performance will need to be separate from the compressor to simulate the various drops in pressure between the compressor and expander.

- ***How should the transient effects of the air supply system be taken into account?***

The transients are a concern when the PR and/or  $\dot{m}$  of the system air volume need to be changed to meet a new system power demand. It appears that the issue is not simply one of altering the compressor performance but rather, the time it takes to alter the condition of the air in the entire system (compressor, air ducts, fuel cell stack, and expander). This is why it becomes important to package the compressor near the fuel cell stack and reduce any need for additional air volume in heat exchangers.

- ***Will air heat exchangers be necessary?*** If the outlet temperature of the air from the compressor is sufficiently higher than the operating temperature of the stack (typically 80°C for pressurized PEM fuel cells) then the air will need to be cooled. This adds to the complexity of the system and is an additional argument to operate at lower PR values (thus reducing the temperature of the air from the compression process).

- ***How should the issue of various ambient air conditions be addressed?*** Air system modeling should utilize input data that is "corrected to reference values" in order to be able to accurately simulate various ambient conditions such as temperature and pressure.

## A PROPOSED METHODOLOGY FOR AN AIR SUPPLY MODEL

This section proposes one possible approach to modeling the fuel cell system air supply. Note that much of the information is *specific to centrifugal compressor technology* (a.k.a. turbocompressor) and that work is needed to create a model applicable to the other technologies considered for automotive fuel cell systems. This section begins with a summary of the important performance parameters followed by an example of how to correct the input data to reference values. Next, the use of performance maps is addressed followed by a discussion of how to utilize the corrected data and performance maps in the model.

### ***Performance Parameters:***

There are several important performance parameters that are necessary for modeling the air supply. The following table summarizes the parameters.

**Table 1. Performance Parameters**

Parameter	Comments
PR	ratio of compressor output pressure to inlet pressure
mdot	air mass flow rate
SR	stoichiometric ratio, ratio of <i>moles of O<sub>2</sub> in the air per second</i> supplied to fuel cell stack vs. <i>moles of O<sub>2</sub> per second</i> utilized at the corresponding stack power level (or fuel consumption rate)
T	temperature
N	motor shaft rotational speed
P	power
$\eta_{\text{comp}}$	isentropic efficiency of compression

Additional notes regarding the power and efficiency follow.

*Power:*

$P_{\text{comp}}$  = electrical power needed for compressor motor

$P_{\text{shaft}}$  = shaft power of the compressor motor

$P_{\text{thermo}}$  = thermodynamic, non-isentropic power of compression, not including mechanical friction irreversibilities

*Isentropic Efficiency (sometimes called "adiabatic efficiency"):*

$$\eta_{\text{comp}} = [\dot{m} * c_p * T_1 * (PR^{(k-1)/k} - 1)] / P_{\text{thermo}} \quad [3]$$

where  $c_p$  = specific heat at constant pressure,  $k$  = ratio of specific heats,  $T_1$  = inlet air temperature, and  $P_{\text{thermo}} = [\dot{m} * c_p * (T_2 - T_1)]$

This definition of efficiency is based on the thermodynamic power of compression including thermodynamic irreversibilities, but not including any mechanical irreversibilities. For accurate comparisons between various air supply technologies, it may be useful to define an "adjusted", or shaft, efficiency where  $P_{\text{thermo}}$  is replaced with  $P_{\text{shaft}}$  (where  $P_{\text{shaft}} = \eta_{\text{mech}} * P_{\text{thermo}}$ ). However, further discussion with the developers is needed to reach agreement, considering developers commonly specify  $P_{\text{thermo}}$ .

***Corrected Data:***

In order to create a model that is flexible enough to simulate various ambient performance conditions, it is necessary to use "corrected variables". The following is an example of how one might correct the data. Note that this is an example for a *centrifugal air compressor* [Reference 2] and the format for the corrected data will vary depending on the technology used.

The corrected variables used are:

$$\Theta = T \text{ (K)} / 288 \text{ K}$$

$$\delta = Pr \text{ (atm)} / 1.0 \text{ atm, } Pr = \text{pressure}$$

$G_1$  = characteristic dimension used for physical scaling (where  $G$  can be length, area, or volume)

$G_2$  = additional characteristic dimension used for physical scaling (when multiple scalars are needed)

$$\gamma_1 = G_1 / G_{ref1}$$

$$\gamma_2 = G_2 / G_{ref2}$$

The format for correcting the performance parameters is as follows:

$$\text{Compressor pressure ratio: } pr_{out} / pr_{in} \quad [4]$$

$$\text{Corrected mass flow: } (\dot{m} * \sqrt{\Theta}) / (\delta * \gamma_1^2) \quad [5]$$

$$\text{Corrected shaft speed: } N / \sqrt{\Theta} \quad [6]$$

$$\text{Corrected shaft power: } P_{shaft} / (\delta * \sqrt{\Theta} * \gamma_1^2) \quad [7]$$

The corrected variables may take the following *general form*:

$$\text{Compressor pressure ratio: } Pr_{out} / Pr_{in} \quad [8]$$

$$\text{Corrected mass flow: } \dot{m} * \delta^{X1} * \Theta^{Y1} * \gamma_1^{Z1} * \gamma_2^{V1} \quad [9]$$

$$\text{maximum allowable: } \dot{m}_{max}(N_{max}) * \delta^{X2} * \Theta^{Y2} * \gamma_1^{Z2} * \gamma_2^{V2}$$

$$\text{Corrected shaft speed: } N * \delta^{X3} * \Theta^{Y3} * \gamma_1^{Z3} * \gamma_2^{V3} \quad [10]$$

$$\text{maximum allowable: } N_{max} * \delta^{X4} * \Theta^{Y4} * \gamma_1^{Z4} * \gamma_2^{V4}$$

$$\text{Corrected shaft power: } P_{shaft} * \delta^{X5} * \Theta^{Y5} * \gamma_1^{Z5} * \gamma_2^{V5} \quad [11]$$

*where the exponents have to fit the data supplied by the compressor developers, and will be unique for each compressor type.*

In the above equations, it is assumed that the actual  $\dot{m}_{max}$  changes with varying ambient conditions. This is a realistic assumption considering a compressor technology may have a physical constraint that creates a single maximum shaft speed ( $N_{max}$ ) regardless of the ambient conditions. In this situation, as the ambient air density alters (due to pressure or temperature changes) and yet  $N_{max}$  remains the same, the output

$\dot{m}_{\max}$  will change. Therefore, equation [9] utilizes a variable, actual  $\dot{m}_{\max}$ , which is a function of actual  $N_{\max}$ .

As seen in Figure 2 below, it is necessary to correct the shaft speed when correcting the mass flow to maintain the inter-relationship on the common performance map.

### ***Performance Maps:***

The data input format is based on compressor performance maps. An example of one of these performance maps is shown in Figure 2, a map that is used for a centrifugal compressor technology [Ref. 3, AlliedSignal]. Figure 3 provides a map incorporating corrected  $P_{\text{shaft}}$  vs. corrected speed [Ref. 3, AlliedSignal].

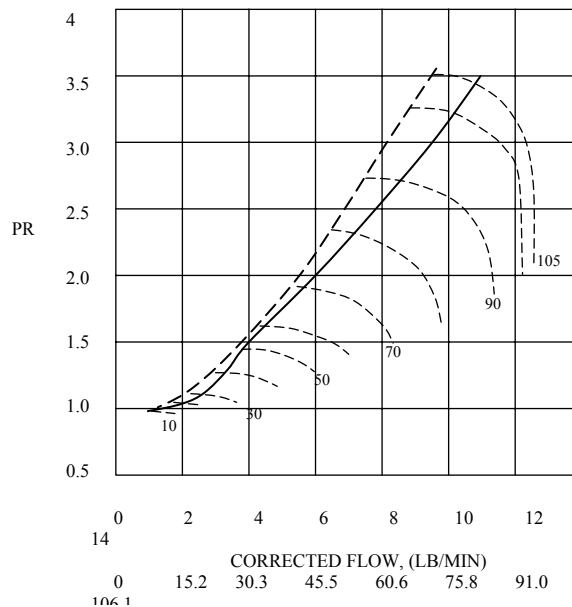


**Figure 2: Pressure Ratio vs. Corrected Mass Flow [Ref.3]**

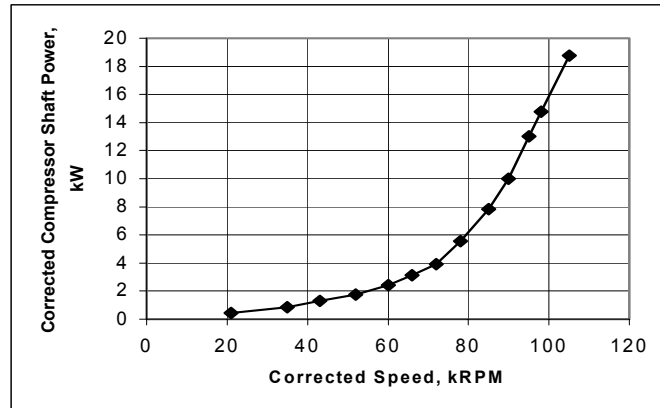


**Figure 3: Shaft Power vs. Mass Flow along the operating line [Ref.3]**

where, in Figure 2, the curved dashed lines that progress from upper-left to lower-right represent constant corrected speed lines (thousands of RPMs: kRPM), the single dashed line represents the surge line, and the single solid line represents the operating line

These maps can incorporate a number of descriptive features. First, the Figure 2 map defines the relationship between pressure ratio, the mass flow of air, and corrected shaft speed. Second, Figure 3 specifies the corresponding corrected motor shaft mechanical power for each PR/mass-flow/shaft-speed combination along the operating line. Third, they can show the limiting ranges of PR and mass flow attainable with the specific compressor technology.

The key modeling problem is how to incorporate the data on performance maps into the air supply model in the FCV code. This will be discussed shortly.

### ***The Air Supply Model:***

A model is needed that has the flexibility to simulate various air supply technologies. This is very useful in determining which technology is best suited for a given fuel cell system and vehicle configuration. Currently, fuel cell system developers are working with a number of different technologies that include reciprocating piston, twin screw,

scroll, and turbo compressor designs. Depending on the technology, the performance maps, and method of correcting the data, may vary. With this in mind, the model should include a section for each type of air supply technology. However, for accurate technology comparison and model consistency, a common set of input and output parameters should be utilized (as defined in Table 1). This also allows for incorporation into the fuel cell system model in a way that is consistent for all the air supply technologies.

For an individual simulation, one type of technology is chosen. Once the ambient conditions for the specific computer simulation run are defined, the air supply model will use this information along with the required  $\dot{m}$  as inputs to "look-up tables" (which includes the compressor performance maps). The output results should be the actual required  $P_{\text{shaft}}$ ,  $N$ , and  $PR$ . With this information, an electric motor map is utilized to determine the consumed electrical power for compression. The consumed power is then used for calculating the fuel cell system *net* power and *net* efficiency. The following example provides insight into much of this process.

### ***Turbocompressor Example***

The following is an example of the results obtainable using the proposed air supply model. The example utilizes the AlliedSignal fuel cell compressor maps shown in Figures 2 and 3. The results of the simulation compare the performance of the same compressor in two distinctly different ambient conditions, Scenario 1 at standard operating conditions (25 °C and 1atm) and Scenario 2 at a high elevation on a hot day (i.e. Denver, CO: 35 °C and 0.8atm). The two scenarios both utilize the same requested

$\dot{m}$  for the fuel cell stack operation but result in different shaft powers, speeds, and PRs. Refer to Tables 2 and 3 for the input values and output results, respectively.

**Table 2: Input values and exponents**

	<b>Scenario 1</b>	<b>Scenario 2</b>
	<b>STP</b>	<b>Denver,CO</b>
<b>Ambient:</b>		
$T_{amb}$	298 K(25C)	308 K(35C)
$P_{r_{amb}}$	1 atm	0.8 atm
$G_1 = G_{ref1}$	1	1
$G_2 = G_{ref2}$	1	1
<b>Exponents:</b>		
$x1, y1, z1, v1$	-1, 0.5, -2, 0	-1, 0.5, -2, 0
$x2, y2, z2, v2$	-1, 0.5, -2, 0	-1, 0.5, -2, 0
$x3, y3, z3, v3$	0, -0.5, 0, 0	0, -0.5, 0, 0
$x4, y4, z4, v4$	0, -0.5, 0, 0	0, -0.5, 0, 0
$x5, y5, z5, v5$	-1, -0.5, -2, 0	-1, -0.5, -2, 0
<b><math>\dot{m}</math> requested (g/s), actual:</b>		
$\dot{m}_{dot1}$	10	10
$\dot{m}_{dot2}$	25	25
$\dot{m}_{dot3}$	40	40
$\dot{m}_{dot4}$	55	55
$\dot{m}_{dot_{max}}$	78.3	60.1

The exponents are based on the actual lab data shown in Figure 2 and utilize the format shown in equations 5, 6 and 7.  $\dot{m}_{dot_{max}}$  is based on an assumed  $N_{max} = 105\text{kRPM}$ .

**Table 3: Output results (compressor only)**

	<b>Scenario 1</b>			
	<b>Pshaft</b>	<b>N</b>		
	<b>(kW)</b>	<b>(kRPM)</b>	<b>PR</b>	
$\dot{m}_{dot1}$	0.23	20.3	1.05	
$\dot{m}_{dot2}$	1.266	45.8	1.29	
$\dot{m}_{dot3}$	3.451	68.6	1.85	
$\dot{m}_{dot4}$	7.178	84.7	2.4	
	<b>Scenario 2</b>			
	<b>Pshaft</b>	<b>N</b>		<b>Increase</b>
	<b>(kW)</b>	<b>(kRPM)</b>	<b>PR</b>	<b>in Pshaft</b>
$\dot{m}_{dot1}$	0.314	21.7	1.09	36.5%
$\dot{m}_{dot2}$	1.74	58.9	1.55	37.4%
$\dot{m}_{dot3}$	4.551	82.7	2.19	31.9%
$\dot{m}_{dot4}$	11.06	98.2	3	54.1%

Note 1: The above data was derived using the operating line on the performance map.  
 Note 2: The shaft power and speed above are the actual, uncorrected data.

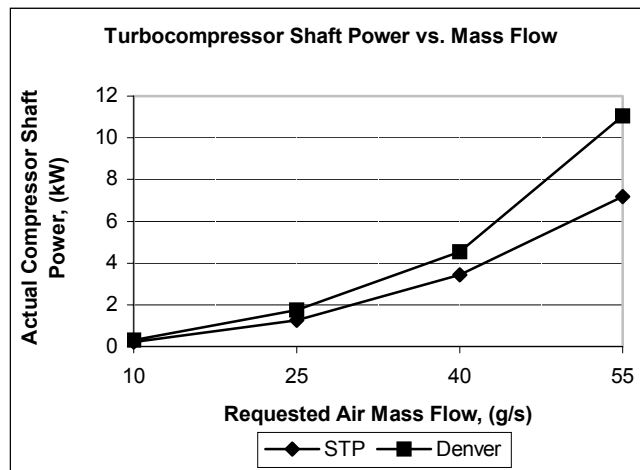


Figure 4: Compressor Shaft Power vs. mdot

### Discussion

The results (shown in Table 3 and Figure 4) reveal that when operating the FCV with the centrifugal compressor at the higher altitude on a hot day, the power consumed by the compressor increased for all the requested mdot values with the largest increase, 54.1%, occurring at mdot4. Additionally, the PR values of Scenario 2 increased for the same requested mdot values with a percentage increase ranging from 3.8% (mdot1) to 25% (mdot4). Close examination reveals that it is the change in ambient pressure that most notably alters the output results. Specifically, the change in  $\delta$  was 20% whereas the change in  $\sqrt{\Theta}$  was only 1.7%. Considering that the air supply is a dominant parasitic loss in the fuel cell system, the magnitude of the differences between Scenario 1 and Scenario 2 is not insignificant.

The results are not surprising. As the ambient temperature increases and the ambient pressure decreases, the inlet air density is reduced thus resulting in less mass flow for the

same shaft speed. In order to achieve the same mass flow in both scenarios, the shaft speed must be increased in Scenario 2. Considering the shaft power is highly dependent on shaft speed, the power consumption increases.

This example was used to illustrate how the performance of the same compressor may change at varying ambient conditions. The model can also be used to compare various compressor technologies. Additionally, several other compressor features will be important in comparing the various technologies. First, the maximum shaft speed and power limits of the particular technology need to be analyzed to determine if the air supply is scaled properly for the application. Second, the air supply technology should be chosen such that it operates near its most efficient performance point over a large percentage of the specific driving cycle (corresponding to fuel cell system power demands). Third, physical size and weight need to be considered when packaging the air supply in the vehicle application.

#### ***Fuel Cell System Results (for the compressor example)***

As mentioned earlier, the fuel cell system performance is affected with the change in the air supply performance. The increased air supply power reduces the net fuel cell system power and efficiency even though the same requested  $\dot{m}$  input values were utilized for both scenarios. It is important to note that as the PR increases for Scenario 2, the gross power from the fuel cell stack is expected to increase. However, the increased gross power may not be significant enough to compensate for the increased compressor power consumption.

Though the details of the fuel cell system model will not be discussed in this paper [Ref.1], the following table shows a few basic results of the fuel cell system under the two scenarios. The table uses the requested mass flow and PR associated with the mdot3 condition (40 g/s) for illustration purposes. It is this integration of the air supply performance into the fuel cell system model that is important to system developers.

**Table 4: Fuel Cell System Results**

	<b>Scenario 1</b>	<b>Scenario 2</b>
Max. Gross Fuel Cell Stack Power	33.5 kW	34.5 kW
Compressor Power - electric	4.2 kW	5.5 kW
Net Fuel Cell System Power	29.3 kW	29.0 kW
Net Fuel Cell System Efficiency @ net system power	38%	37%
* Note: the PR associated with mdot3 (40g/s) was:	1.85	2.19

The results in Table 4 confirm several expected trends. First, the gross power increased for Scenario 2 due to the higher PR value. However, after taking the increased compressor electric power into consideration, the net system power and efficiency decreased. Overall, the net system efficiency dropped by one percentage point.

### ***Further Development***

The use of an expander/turbine in the model was not discussed but will be incorporated at a later time by utilizing a similar methodology. A performance map will be necessary that defines actual recovered shaft power for the given fuel cell stack exhaust gas conditions.

Additionally, as mentioned previously, transient delays due to the time it takes to alter the pressure in the system will be important to study. A next step will be to incorporate a model of the physical volume of air in the piping and internal to the components in order to simulate the pressure drop characteristics and the transient delay.

## **CONCLUSION**

Overall, it has been pointed out that a realistic air supply model is necessary for use in fuel cell system development. There are two prominent reasons for this. First, to accurately analyze fuel cell system results, the power consumption of the air supply needs to be subtracted from the gross output power from the fuel cell stack. Second, to maximize the performance of a particular FCV system configuration, it will be necessary to compare various air supply technologies in the system model.

With that as motivation, this paper has provided a methodology for creating a flexible and realistic air supply model. The model utilizes air supply performance maps incorporating pressure ratio, corrected air mass flow rate, operating efficiency, corrected motor shaft speed, and corrected motor shaft power. These are incorporated into the simulation model as table look-ups.

As a final note, it is important to re-iterate that this research needs air supply developer feedback to determine if this is the best method for incorporating their particular compressor/expander performance characteristics into the simulation.

## ACKNOWLEDEMENTS

The work presented in this paper is supported by the Fuel Cell Vehicle Modeling Project at the Institute of Transportation Studies, University of California, Davis. The modeling process utilizes the Matlab/Simulink programs.

## REFERENCES

1. D.J. Friedman and R.M. Moore, *PEM Fuel Cell System Optimization*, Electrochemical Society Symposium, November 1-6, 1998.
2. W.W. Bathie, Fundamentals of Gas Turbines, 2<sup>nd</sup> Edition, John Wiley & Sons Inc., 1996, pp242-245.
3. "Fuel Cell Turbocharger", AlliedSignal Aerospace, presentation to US DOE and Argonne National Laboratory, Wash. D.C., June 25, 1998.